KTeV TRD DESIGN REPORT

Y. B. HSIUNG, J. C. KRIDER, V. PESKOV,
E. J. RAMBERG, R. TSCHIRHART
Fermi National Accelerator Laboratory

G. E. GRAHAM, N. SOLOMEY, Y. W. WAH,
R. WINSTON, E. D. ZIMMERMAN
Enrico Fermi Institute, The University of Chicago

February 9, 1994

A description of the final design of the KTeV transition radiation detector is presented. The necessity for a TRD particle ID system in KTeV, the final TRD design, electronics requirements, cost estimates and construction schedule are explicitly laid out.

Contents

Chapter 1

Physics Justification for the KTeV TRD System

The purpose of the KTeV TRD system is to provide electron/pion rejection independent of the CsI calorimeter. In particular, Ke3 background to the signal $K_L \rightarrow \pi^0 e^+ e^-$ will be rejected at a single event sensitivity level of $\approx 10^{-12}$. The best limit on this decay mode is dominated by this background at the 4×10^{-9} level. If 10^{-12} sensitivity is to be reached, then rejection at KTeV must be better by about three orders of magnitude than in E799-I. The CsI calorimeter provide pion rejection five to ten times better than the lead glass calorimeter used previously. A factor of 200 or more in pion rejection must therefore come from the TRD system planned for KTeV rare kaon decay experiment E799-II.

Trigger rates can be reduced by a fast TRD trigger system, allowing higher sensitivity to rare decays. Preliminary work has shown this reduction to be necessary in E799-II. During E799-I, the 4 track trigger was prescaled by a factor of 10 and the Dalitz trigger by a factor of 16; this could be improved with electron identification at level two trigger selection.

The TRD system will also find applications in E832, distinguishing between the two charged pion decay of the kaon and Ke3 events. The hyperon decay experiment will also make use of the information from this TRD system to identify the electron of the Lambda beta decay and other forbidden Hyperon decay searches.

Chapter 2

Design of the KTeV TRD

General considerations for designing the KTeV TRD system are discussed and the final detector design is described. This design was based on the capability of the wire chamber facilities at Fermilab, as well as on many laboratory tests and two beam tests simulating conditions expected at KTeV.

2.1 Description of E799-I TRD

The KTeV TRD project is a continuation of the TRD project of E799-I. Three wire chambers were constructed for that experiment. Figure 2.1 shows the design of the chamber used in E799-I; this design included a conversion region for X-rays in front of a MWPC. Data from these chambers, shown in Figure 2.2, show a distinct difference between signals from electrons and pions.

Variations in the position of the mylar cathode window caused changes in gain across the full surface of these detectors, making it difficult to use the signals coming from the chamber. A long drift time arising from the conversion gap required a gate width of 500 ns. Any reduction of this time would alleviate background problems by reducing the number of accidental hits. The dense xenon gas mixture caused a substantial bulging in the windows of the TRD, on the order of 2 cm or more. This distorted the X-ray sensitive conversion gap, causing the varying gain non-uniformities. The new TRD design for KTeV eliminates these difficulties, and aims for long term stability of detector operation. A recirculating gas system was built for the E799-I TRD system, and a modified version of this system will used in KTeV.

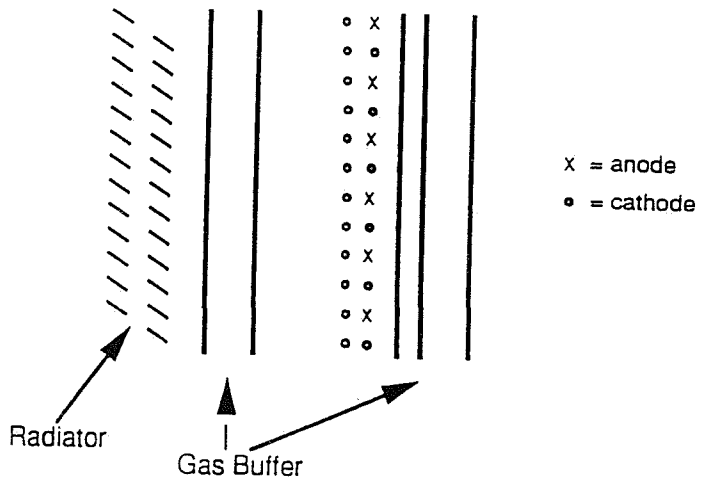

Figure 2.1: Design of the TRD chamber used in experiment 799-I.

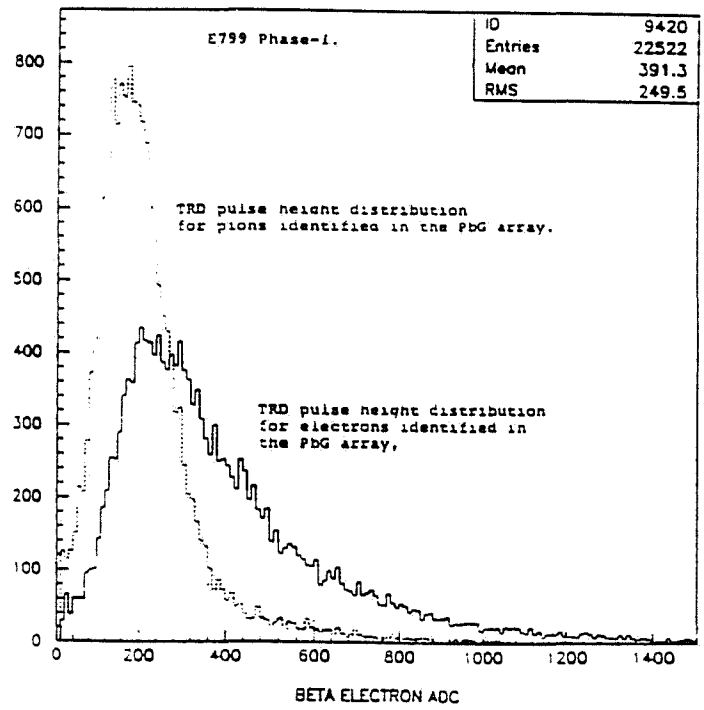

Figure 2.2: A comparison between electron (solid) and pion (dashed) signals from E799-I TRD.

2.2 General design considerations for a large area TRD

There are several factors which make it difficult to construct a TRD for use in KTeV. The main difficulties are the fact that a large aperture is needed to accommodate decay products, on the order of 2x2 m^2, and that the rate of charged tracks through the face of the detector will be reasonably high, 10 kHz/cm^2 or >100 kHz/wire near the beam region. In KTeV there may be a non-negligible contribution of charge deposited from accidental hits unless the gate width is small and the detector is finely segmented. This consideration has led to a chamber design which has multiple layers of MWPCs with fine segmentation in the longitudinal direction, thus keeping the drift length small in all directions.

The large area windows, if unsupported, would bulge from the static load of a slight gas over pressure, as well as have a gravitational bulge near the bottom of the detector due to the dense xenon gas mixture in the active volume. This bulge would lead to changes in gain across the face of the detector if the window were used as a cathode. It would also result in a varying X-ray detection efficiency across the face of the chamber. A buffer volume containing a gas mixture whose density is chosen to match that of the xenon gas mixture will be used to help support the entrance window. This will keep the inner aluminized window flat to within 100 microns. The entrance window that separates the radiator from the X-ray sensitive gas was designed to be as transparent to X-rays as possible. The buffer gas is still the most X-ray absorbent component of the entrance window, but it is at a level which is acceptable for the X-ray energies expected. The gaseous support mechanism of the inner window has been tested, with satisfactory results, over a period of several months. Such a design requires that changes in atmospheric pressure be accounted for by an active pressure compensating gas flow system so as to prevent large changes in gain and efficiency.

The radiator for the KTeV TRDs will be a polypropylene fiber mat. The mat will have a dry gas flowed through it to keep atmospheric contaminants and humidity to a minimum. The radiator will be cut away in the beam regions to minimize unwanted beam interactions. The wires inside the chamber over the beam hole region will be deadened with a piece of mylar, so the high rate environment of the beam hole will not affect the performance of the chamber.

The design of the individual TRD modules and whole system was guided by the X-ray transition radiation detector simulation software. The transition radiation simulation is based upon well known formulae of classical electromagnetic theory applied to the special case of ultra relativistic particles. For a given foil radiator and particle energy, a transition radiation spectrum was simulated. The X-rays are

propagated through each specified region of the TRD using Monte Carlo techniques. Ionization energy loss of particles in the TRD is not modeled. Instead, calculation of e/π rejection depends on measurements of the charged particle energy loss in the TRD prototypes. It has been found that the rejection factor is quite sensitive to the exact form of the high energy tail of the ionization energy loss distribution. Thus, measurements of this distribution play an important role in the design of the KTeV TRD.

Using the full simulation of the final design, and using the best estimation of ionization spectrum available, a factor of about 350:1 in pion rejection was obtained by using a 2-dimensional likelihood analysis for a 8 chamber system. Clearly, the performance of the TRD in the noisy environment of the beam line may be significantly worse, but these estimates indicate that the TRD will succeed at identifying pions and electrons at the required level. Here the rejection factor is quoted for 90% electron efficiency.

2.3 TRD chamber design

A TRD plane consists of a gaseous X-ray detector volume, with a radiator that generates TR X-rays, and a highly transparent window to couple the radiator to the X-ray detector. Several other major support systems such as gas system and electronics are also essential to the proper operation. Each of these major components of a single detector volume will be reviewed and its impact on the final design.

2.3.1 X-ray detector design

A 6 mm anode-to-cathode gap was chosen to minimize the charge collection time. It was considered risky to build and stably operate a large wire chamber with a gap size smaller than 6 mm. Since 20 mm or more of Xenon was desired for the conversion of X-rays, this requires two back to back MWPC planes. Within each plane, the anode wire spacing was chosen to be 5 mm. It is important to keep the tolerances on the cell size to 50 microns, corresponding to a 10% variation in gain. Since the entrance window cannot meet those tolerances under a gas pressure load, a layer of wires will be used as the cathode. The gain stability provided by wire cathodes allows the aluminized mylar window to be held at a few hundred volts above the cathode wire voltage, providing a small drift region at the front of the chamber that will collect electrons from converted X-rays. This region will be as small as possible, given the timing constraints. Tests have shown the gain under this configuration to be stable.

Originally, the concept of multiple MWPC layers was conceived as a means of improving the charge collection time. However, results from the Brookhaven

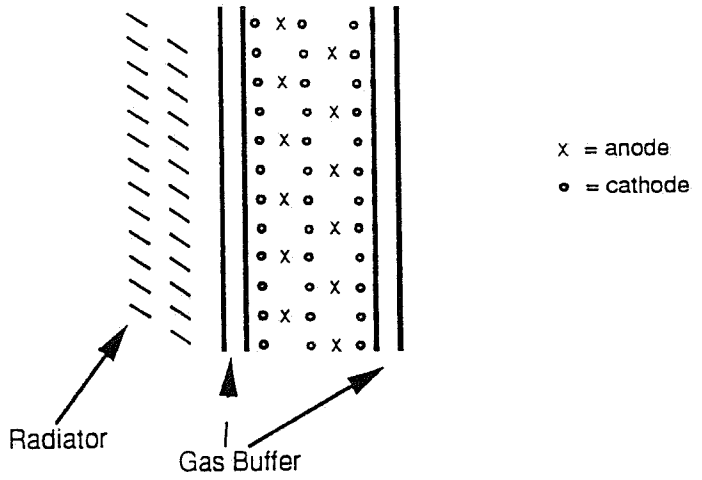

Figure 2.3: Final design of the new TRD chambers to be built for KTeV.

beam test show that having independent multiple layers of ionization planes allows for greater pion rejection. To take advantage of this would only require additional electronics. Therefore it was decided that each chamber would consist of two MWPC layers, for a total of 27 mm of xenon gas mixture. The chamber cell design is shown as Figure 2.3.

Because of the buffer volume, the inner window will be stable with respect to all atmospheric changes such as pressure variations. The buffer volume also acts as a slow filter against atmospheric contaminants such as oxygen and water vapor. Some TR X-rays can however be absorbed by the buffer gas. Therefore, its length will be minimized to 1 cm. The buffer volume will have its own gas recirculating system. The recirculating gas system already built for E799-I will be modified and used for the active gas volume.

Size of the TRD

All TRD modules will be the same size, for ease of construction. We assume the last TRD module will be placed right in front of the H and V trigger scintillation banks. Then the half width of the inner aperture of the TRD needs to be:

$$X_{\rm TRD} = [(Z_{\rm H,V} - 155.2) \cdot \tan\theta_{\rm ray}] - 0.1796 \text{ m} = 1.0423 \text{ m}. \qquad (2.1)$$

where $Z_{\rm H,V} = 184.000$ meter, $\theta_{\rm ray} = 42.4$ mrad is the maximum angle that can be drawn from the beam spot at the end of the decay region (155.2 m) to the CIA, and 0.1796 meter is the half width of the x-projected beam hole size at Z=155.2. Note that the half width transverse size (x,y) of H,V and CIA outer edge are (0.9500,

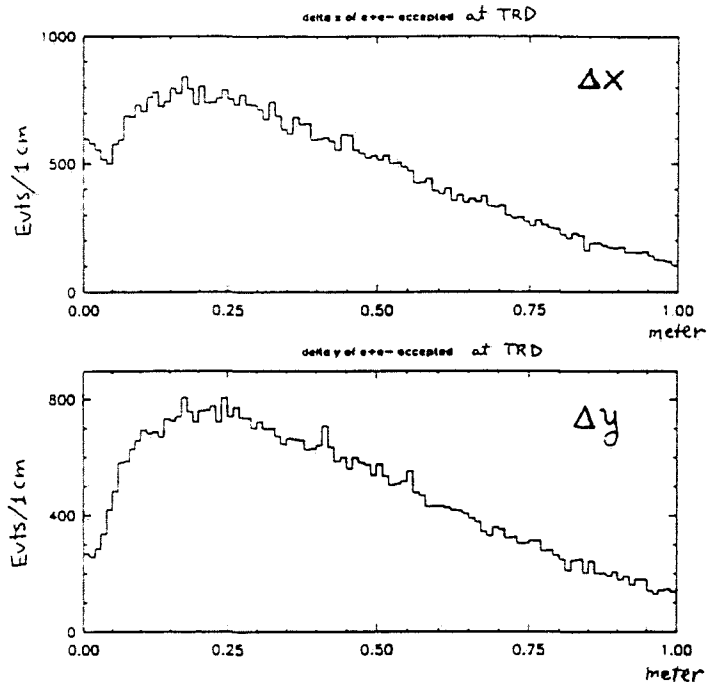

Figure 2.4: Monte Carlo events of the separation in X and Y between the two charged tracks.

0.9500) meters and (1.1009,1.1009) meters respectively. Since the apertures of SA4, DC4, H,V, CIA, and CsI are all squares, the TRD apertures will also be square. Thus, the TRD inner frame size has to be at least 2.0846 meter in both X and Y. The final TRD design contains an inner aperture of 84 inches, or 2.13 meters.

From a Monte Carlo analysis of the $K \rightarrow \pi^0 e^+ e^-$ mode, Figures 2.4 and 2.5 show the position distributions of the electron pair and the inter-track distance distribution on the TRD. The decay region was from 80 to 160 meter, with the generated kaon momentum between 20 and 220 GeV. Cuts were $M_{ee} > 100$ MeV, four clusters found with cluster threshold above 1GeV, and $E_t > 30$ GeV. The analyzing magnet was assumed to have a 100 MeV P_t kick, and the TRDs were located 2 meters upstream of the CsI array. From the Δx distribution, discarding events with tracks closer than 3 cm, the largest summation distance in our wire summing scheme, corresponds to less than about a 5% event loss, which is acceptable. The Monte Carlo track position distributions show there is little need for a transverse sensitive fiducial area larger than 1.8 x 1.8 m^2. Wires will be strung across the entire inner aperture, but data will be read only from the central 1.8 m of wires.

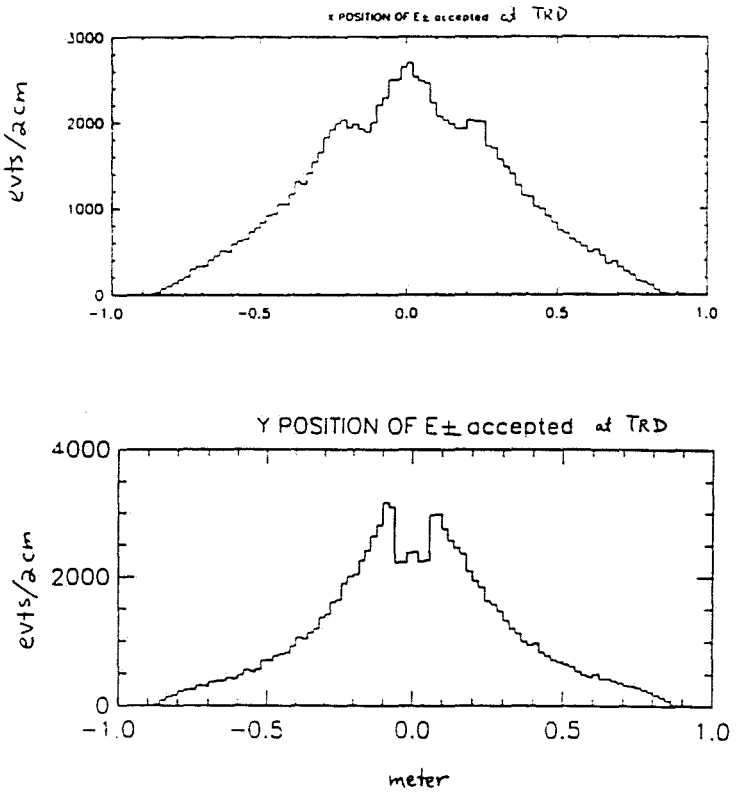

Figure 2.5: For Monte Carlo events, the position of the tracks at the location of the last TRD.

Rates in the TRD chambers

It was assumed conservatively that there would be no improvement in the accidental rate from E799-I. When analyzing hit distributions of Drift Chamber 4 from the accidental triggers of E799-I, it was found that the center portion of the chamber had about twice the rate in both x and y view relative to the edges. From E799-I scaler data, with an intensity of 1.44×10^{12} protons per pulse, the 1B, 1C, MU2, and MU1 rates were: 6.88×10^7, 8.01×10^7, 4.85×10^7, and 6.55×10^7 per spill, respectively. If the 1B rate is taken as the estimate, with its surface area of 2×2 m^2, the average rate of hits during the spill would be $(6.88 \times 10^7)/(23\text{sec} \cdot 200\text{cm})$ = 15 kHz/cm. This corresponds to 67 μs between accidental hits per cm. Since the duty factor of the beam can be on the order of 2, the instantaneous rate can be as high as 30 kHz/cm (one hit per 33 μs). Scaling up to the presumed KTeV rates of 5.0×10^{12}, this gives about 100 kHz/cm (one per 10 μs). However, a fraction of the rate is in the beam hole regions, where the TRDs will have deadened wires. Events here won't contribute to the accidental hit problem. An estimate for the rate in the beam holes can be obtained from the counts in the beam counters in E799-I, which show that fully 30 % of the rate in the scintillator banks can be attributed to the two beam holes. That brings the estimated average rate of hits in the active area down to about 70 kHz/cm (one per 14 μs). If the rate near the beam holes are on the order of twice this value, then there will be 7 μs between charged track crossings per cm in the KTeV TRDs.

Number of channels

It is clearly desirable to minimize the number of accidental hits on a given wire. Reading out every wire, with a 5mm pitch, would indeed minimize the probability of seeing an accidental hit in the same wire as the track to be identified. However, this would require 5760 channels of data readout, the cost of which is currently prohibitive. Therefore, some type of wire summing scheme was necessary.

It will be difficult to get the gate width below 250 ns because of the drift time of at least 150 ns and a pulse width of comparable duration. To bring the level of accidental activity down near the level of a few percent, this would imply that we must read out at most every 1 cm near the center: 1.0(250 ns/7 μs) = 3.6%. As indicated above, an analysis of E799-I accidental triggers indicates that the central portion of the detector receives on the order of twice the accidental rate as the outer portion.

Every other wire will be summed, thus forming an effective pitch of 1 cm in the central 60 cm of the detector covering the two beam hole region. Summing groups of 4 wires in the outer regions will give an effective pitch of 2 cm. This

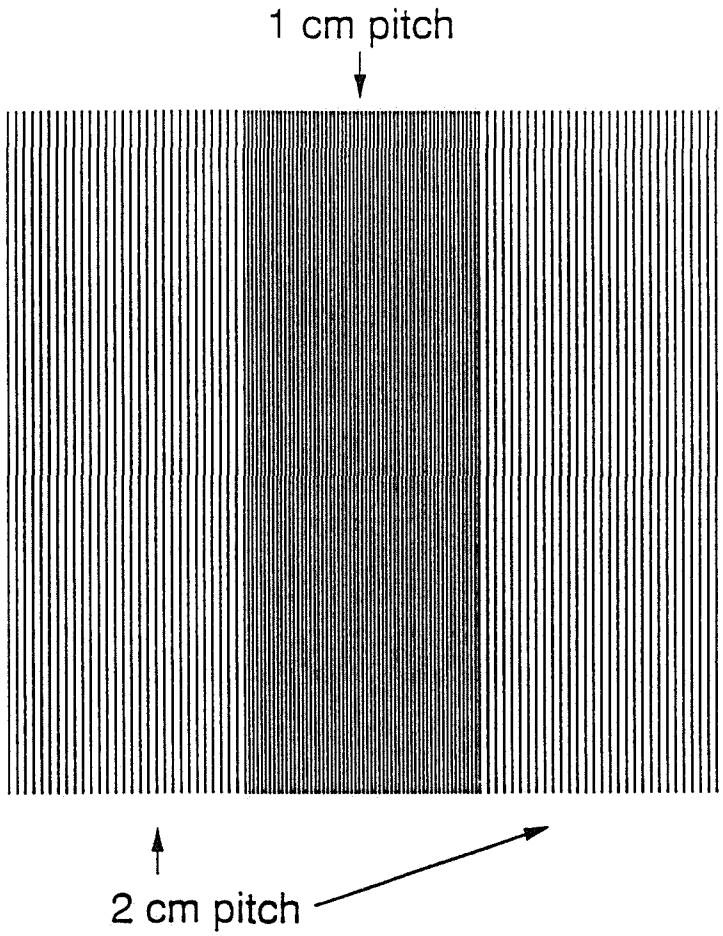

Figure 2.6: The wire summing scheme for the KTeV TRDs.

gives a total of 112 wires/plane, or 224 wires/chamber. For 8 chambers a grand total of 1792 ADC channels are needed. This fits within the 2000 channels of FERA ADCs that have been reserved for the TRD, leaving 5% of the channels available for contingencies. Figure 2.6 shows the wire summing scheme. The signals will be summed with special connectors that attach to the readout cards on the chambers. To change the wire summing scheme, it can be done easily by simply changing the configuration on these connectors.

TRD wire geometry

Figure 2.7 shows the response of a single wire cell of a TRD prototype chamber to a collimated beta source for different source positions. One concern has been that, even with a wire cathode plane separated from the entrance window, movement of the window may cause changes in gain. The large prototype test chamber was used to show that, in fact, there is no significant gain variation under the maximum expected window displacement ($\approx 100\mu$m). Figure 2.8 shows the change in gain under a 100 μm movement of the window as a function of the voltage between the window and

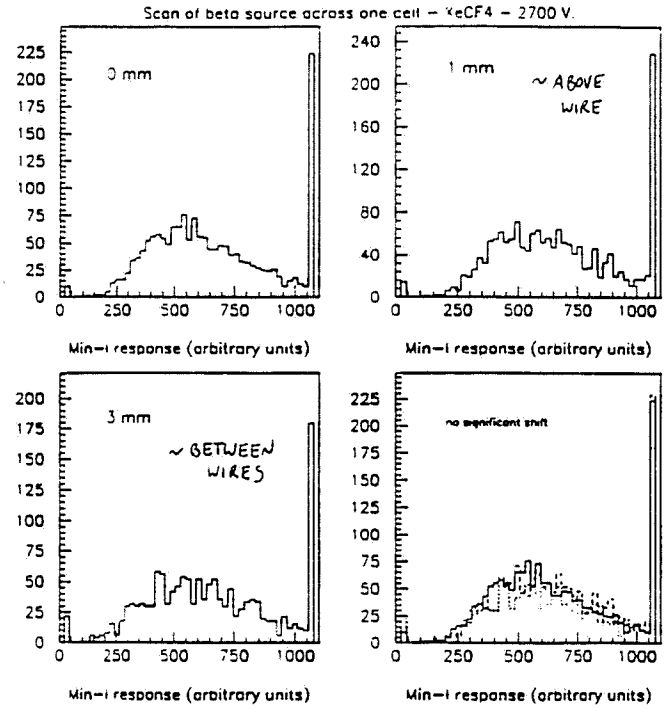

Figure 2.7: The response of a test chamber to a collimated beta source for three source positions the wire chamber cell.

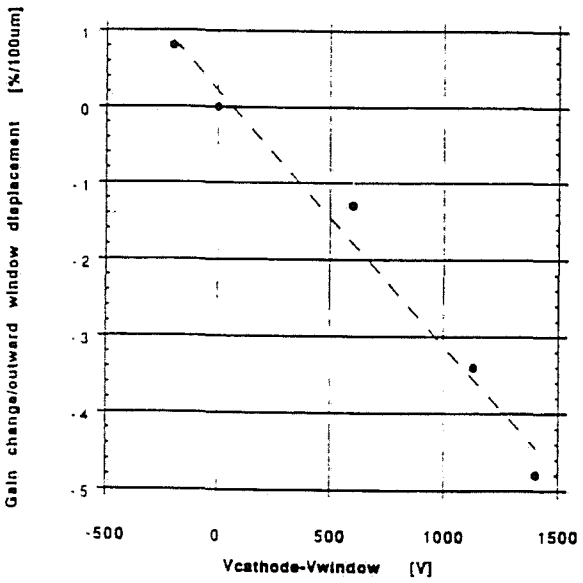

Figure 2.8: The percentage change in gain for an inner window movement of 100 microns, as a function of voltage on the inner window.

cathode wires. When the window is run at 200 volts above the cathode, a 100 μm displacement of the window results in a 1% gain variation, an acceptable instability compared with the 10% anode-cathode gap tolerances.

All wires will be oriented in the vertical direction. Since the magnet kick is in the horizontal plane, the acceptance for charged decay modes which tend to have closely spaced tracks would be degraded if the wires were also horizontal. Also, because the two beams will be separated horizontally, a reduction in accidental rates will result if wires are oriented vertically rather than horizontally.

Electric field calculations have been done for the proposed TRD wire geometry: the dashed lines in figure 2.9 are equipotential and the solid lines are the trajectories that a test charge placed on the surface of the entrance window would take to the amplification region around the anode wires. In KTeV, where a short collection time is a necessity, the field configuration with anodes in line with the cathodes is more advantageous; charge from the drift region is collected in less time. Another benefit to having the anode wires directly behind the cathode wires is that the amplification regions are better shielded from effects due to window displacement.

We have decided to shift the location of the anode wires between the front plane and the back plane by one-half cell (one cathode wire spacing). In this configuration,

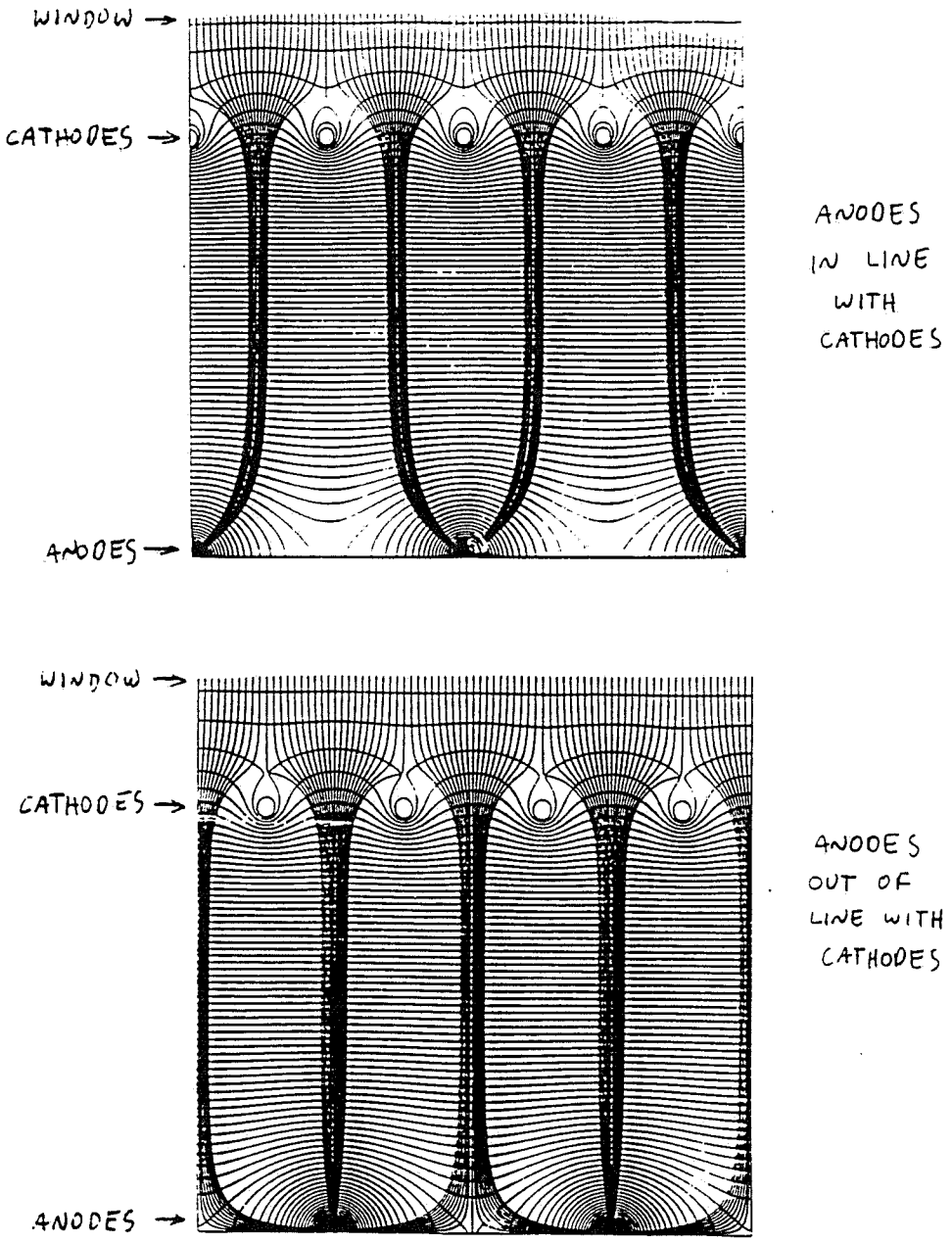

Figure 2.9: Electric field calculations for two wire geometries: a) anodes in line with cathodes, and b) anodes spaced between cathode wires.

some accidental activity will occur in different cells in the front and back planes. This can improve rejection values by making one of the planes free of accidental activity.

TRD gas requirements

Active gas properties Table 2.1 shows drift speeds for various xenon mixtures at an electric field strength of 2 kV/cm. A Xe/CF_4 mixture can be slightly faster than Xe/CO_2. Another advantage of CF_4 is that this molecule does not become absorbed by the various filters in the gas system, as CO_2 can, thus changing the gas composition. Figure 2.10 shows a comparison of the timing of the signals from a triggered X-ray source in a test chamber for various considered gas mixtures. An advantage of CO_2 over CF_4 is that the former has better energy resolution, as shown in figure 2.11. Freon gaseous such as CF_4 and C_2F_6 are electronegative and can absorb electrons before they reach the anode wire causing a loss of X-ray efficiency. Both the loss of energy resolution and the absorption of electrons can cause a drop in X-ray detector performance.

The rejection factor in any TRD system is a function of two physical phenomena: high yield transition radiation production with efficient detection, and ionization energy loss. The effect of ionization energy loss can fake a transition radiation signal and therefore reduce the rejection power. In producing a good TRD it is also necessary to reduce the ionization energy deposited with the TR X-rays as much as possible. One way of reducing the ionization energy loss is to replace a percentage of the Xenon in the detector with a gas relatively low in ionization. Helium is ideal in this respect, but one practical candidate is Neon, because its total ionization is only 39 ion pairs/cm. It also has acceptably low permeability through the chamber windows. By comparison, Xenon has a total ionization of 307 ion pairs/cm. Studies of gas mixtures are currently underway. The decision on the exact gas mixture to be used does not impact significantly the design of the TRD chambers and will be determined later.

Description of the gas system A modified recirculating xenon gas system provided by the Fermilab Physics Section for the E799-I wire chamber transition radiation detectors will be used for the KTeV TRD system. The system provides for: mass-flow gas mixing control, 2 mtorr pressure control, mixture re-circulation, partial online re-purification and recovery of contaminated mixtures that cannot be purified online. Signals from various mass flow and pressure transducers are used to operate mass flow controllers and to generate limits and alarms in interlock hardware which controls automatic valves. The system compensates for changes in

Table 2.1: Gas speeds for various xenon mixtures

Gas mixture	Drift speed (cm/μ sec)
80/20 Xe/CH_4	2.5
80/20 Xe/CO_2	4.5-5
80/20 Xe/CF_4	6.-6.5

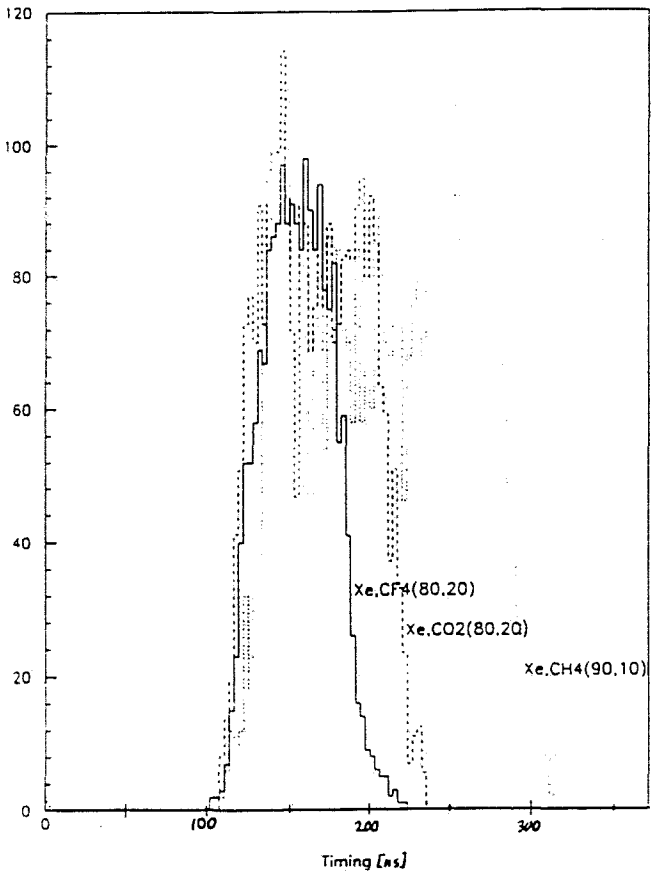

Figure 2.10: Charge collection timing in a test chamber for various gas mixtures.

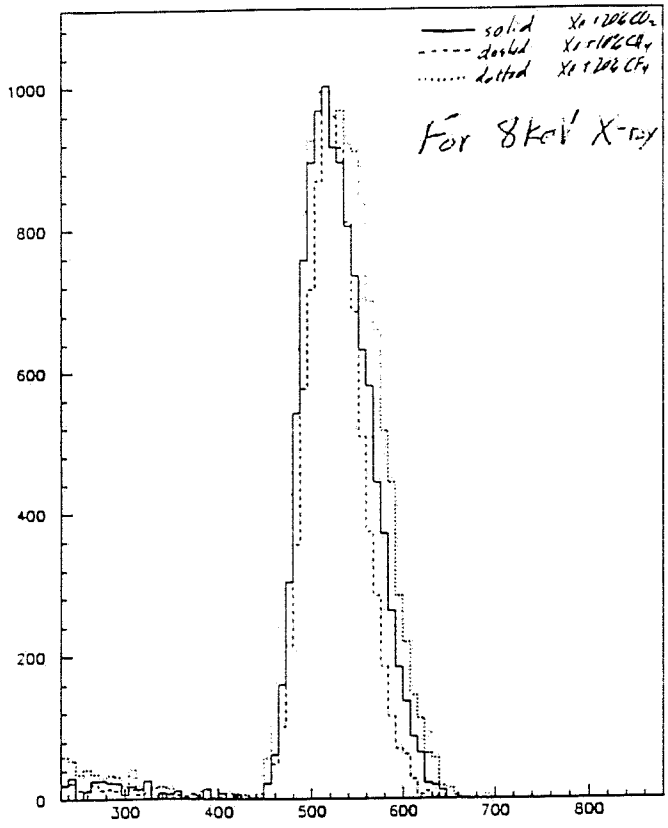

Figure 2.11: Resolution of pulses in a test chamber for various gas mixtures.

atmospheric conditions and for system leaks within specified limits, and it automatically shuts down if these limits are exceeded. Molecular sieves and an oxygen reagent are used to limit the buildup of water and oxygen. Excess or contaminated gases can be diverted to cryogenic recovery tanks for recycling by a commercial supplier. This system will be used for the active gas volume in the 8 chambers. Another simpler gas system will be built for the buffer volumes where the requirements and hence cost for this system will not be nearly as stringent as for the active volume.

A constant gas volume and differential pressure across the windows is accomplished by pneumatic valves controlled by relay logic, which automatically transfer gas between the recirculating system and a reservoir to maintain this balance. Fresh makeup gas is also automatically added when needed.

The recirculating and pressure control equipment consists of a master control module, a circulating pump, pressure and flow control and monitoring, air-actuated automatic valve control, oxygen monitoring and purifiers. The system flow diagram is shown in figure 2.12. Stainless steel plumbing, quarter turn diaphragm valves and bellows-sealed air actuated and needle valves are used throughout the system to minimize contamination. Wherever practical, system joints have been welded together. The remaining connections employ VCO type O-ring seals or VCR metal gasket seals to minimize leaks

The chamber windows are highly permeable to water vapor and have significant permeability to oxygen and nitrogen, the three principal atmospheric gases that degrade performance. Concentrations of 1% nitrogen or a few hundred ppm of water vapor or oxygen are each expected to reduce chamber gain by about 10%. The recirculating gas is passed through a molecular sieve to remove water vapor, and through an oxidizable reagent to remove oxygen. A monitor has been installed to measure the oxygen concentration at any one of four manually selected points in the system.

2.3.2 Entrance window design

The entrance window into the active volume of the X-ray detector is crucial to the operation of a TRD. The design for KTeV is a gas buffer volume holding the window making contact with the active gas volume flat, but this window will not be used as the cathode for the MWPC. The transmission of this window is designed to be highly transparent from 4.5 keV, the threshold of the radiator X-ray production spectrum of polypropylene. The performance of this design was tested in the lab with a triggered X-ray source and was shown to perform close to the calculated expected values, see Figure 2.13. The inner window also requires it to be highly stretched to resist building due to slight pressure differences and should also be as

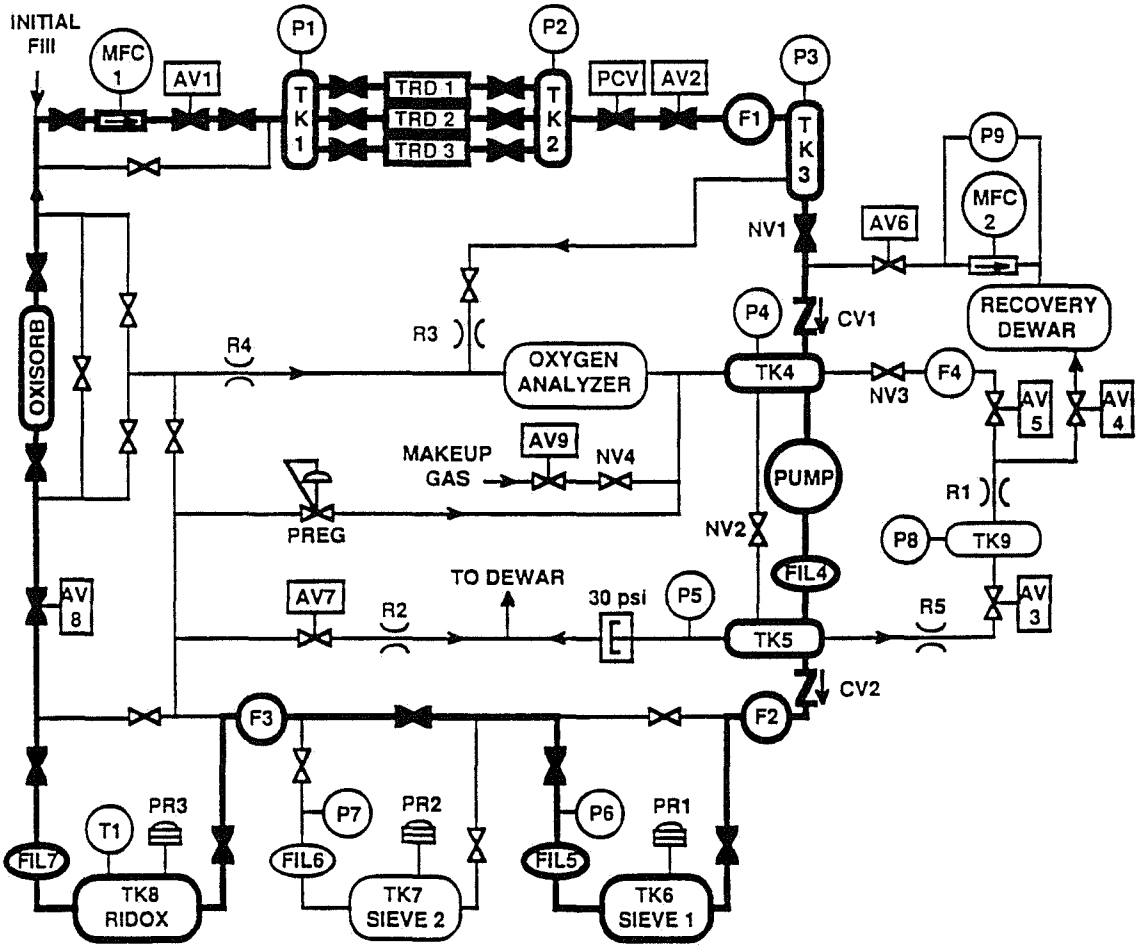

Figure 2.12: Flow diagram of the TRD gas control system.

impermeable as possible, placing high demands and attention during construction.

Mylar window requirements

A new mylar window has been stretched substantially more than the windows used in the E799-I TRDs. Windows on a prototype chamber have been stretched and mounted at a tension of about 10-15 lb/in. Figure 2.14 shows a comparison of this window position vs pressure differential with those of the old TRDs from E799-I. An improvement of a factor of 6 in window stability, or 20 μm/mTorr differential pressure, seems reasonable. With the gas system able to deliver a pressure stability of 1 mTorr or so, the windows should be stable to 100 microns or better. As discussed below, long-term testing of these windows shows this to be the case. A dedicated facility for stretching mylar for the KTeV TRDs exists in the Muon Lab.

Studies have also been performed on the long term loss in tension, or 'creep', in stretched mylar. Figure 2.15 shows that a third of the tension can be lost in stretched mylar over a very short period of time (approximately 500 minutes). After this period, the loss of tension is minimal (15 % over a six-month period).

Contaminants leaking into the active volume from either the buffer gas or the atmosphere have the effect of decreasing the overall gain and energy resolution of the chamber. To counteract this effect, a recirculating gas system has been engineered which removes contaminants such as oxygen and water with filters. To determine whether this system can manage the permeation of contaminants across the large area windows, a facility was constructed in Lab 7 to determine leak rates through plain and aluminized mylar for various gases. Table 1 presents the results of measurements of the permeability of mylar to several relevant gases.

For a TRD system consisting of 8 chambers, each chamber having two windows, it was possible to estimate the load on this recirculating system. Table 2 shows the total gas loss or contamination for the entire TRD system. A pressure differential of 1 atm is assumed in each case. Clearly water vapor is the largest potential contaminant. A possibility exists that Aclar will be added as an extra window on the back of the chamber, which effectively shuts out water vapor permeation on that area. It cannot be put at the front of the chamber because it blocks X-ray transmission.

Gas buffer volume

The buffer volume should have a safe gas that is X-ray transparent and a density on the same order of the chamber gas containing mostly Xenon some choices are: C_2F_6 (ρ_{Xe}= 5.4 g/liter; $\rho_{C_2F_6}$= 5.7 g/liter). It can be mixed with an appropriate amount of quench gas to maintain the same density as the active chamber gas. Another

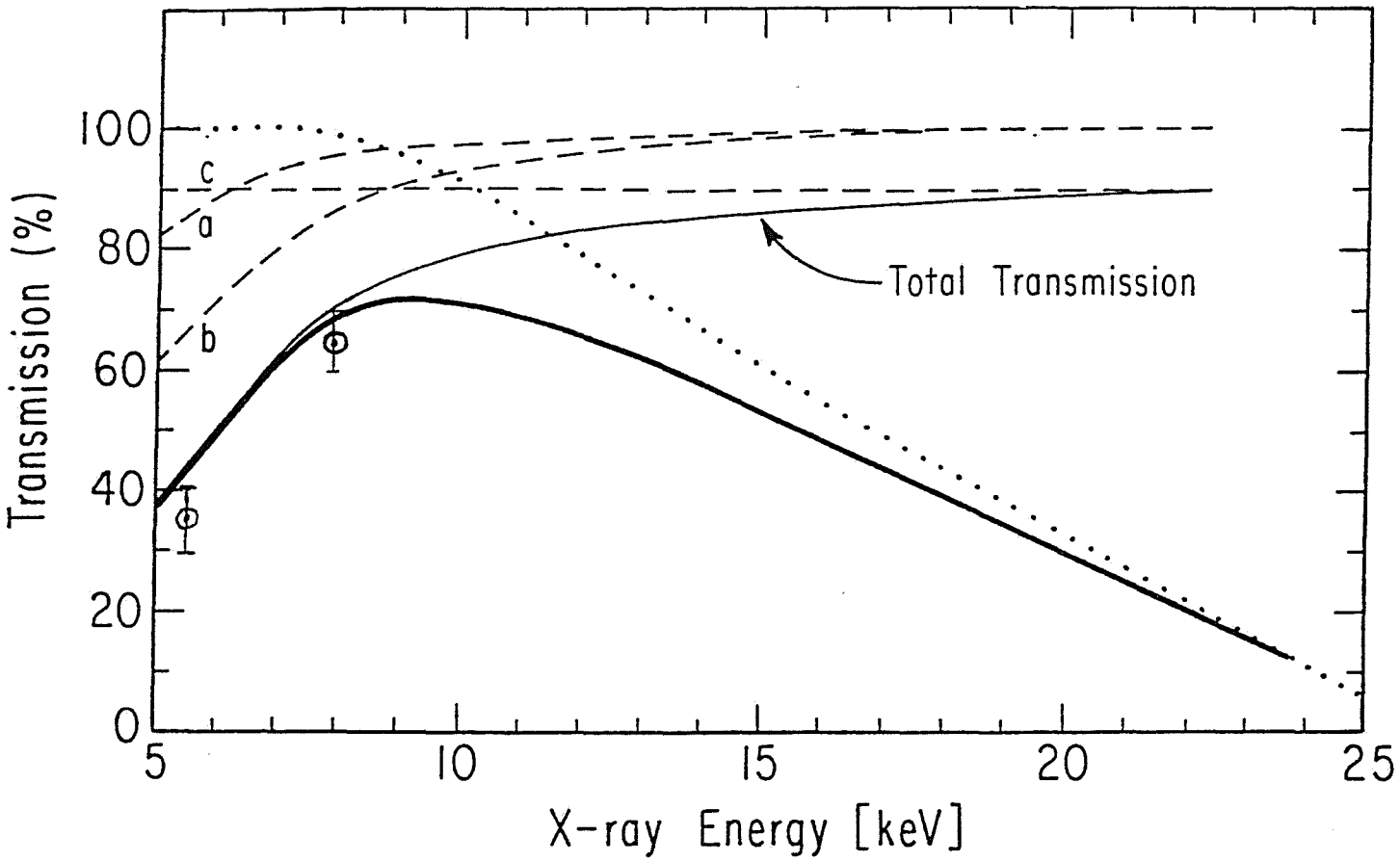

Figure 2.13: Calculated sensitivity of a single detector with the final double flow mylar foil entrance window design. Net sensitivity is shown as the heavy sold curve. The dashed curve a) is the two layers of mylar foil, b) is the 1 cm of heavy buffer gas, and c) a fix wire geometry entrance. The dotted curve it the absorption of X-rays. Two points were measured and are plotted as circles with error bars, and are in agreement with the calculated curve.

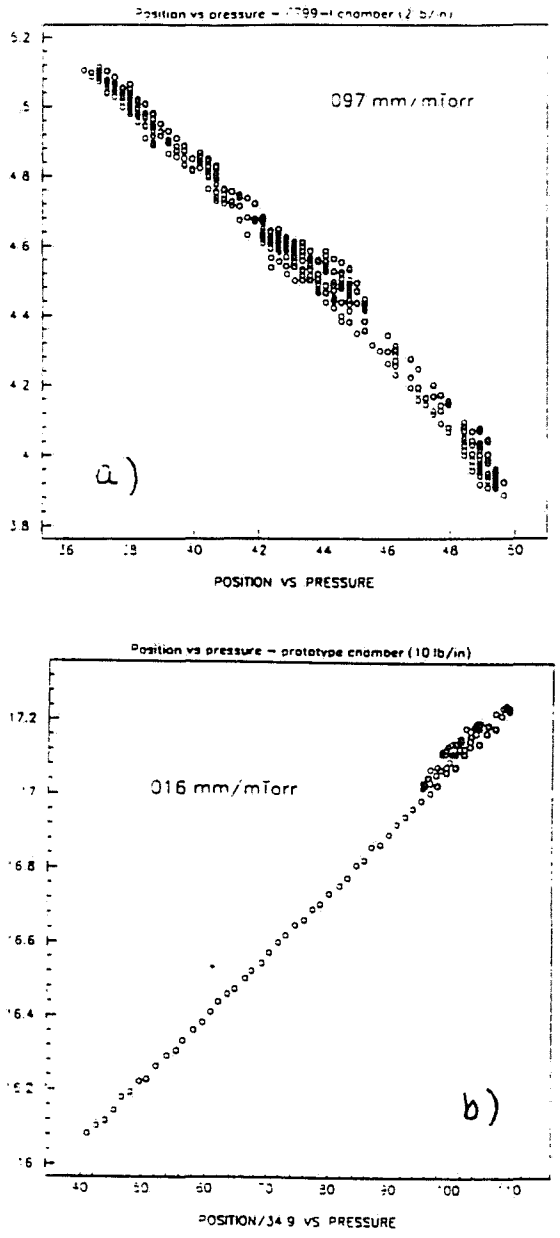

Figure 2.14: Sensitivity of mylar stretch to pressure differential for a) E799-I chamber windows and b) KTeV prototype chamber window.

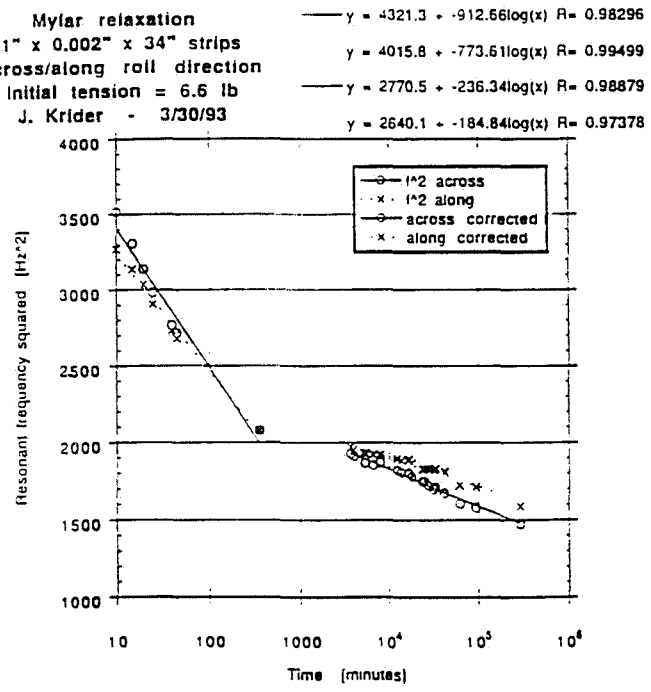

Figure 2.15: Relaxation of tension in mylar over an extended period.

Table 2.2: Mylar permeability to several gases. Units are cm^3 / (day · 100 in^2· atm)

Gas	Plain Mylar	Aluminized Mylar
H_2O	5900	330
CO_2	19	1.26
O_2	2.9	–
N_2	.54	.14
Xe	.095	–
C_2F_6	$< .0076$	–
CF_4	$< .00076$	–

Table 2.3: Gas permeation in TRD system of 8 chambers. Units are liters per day.

Gas	Plain Mylar	Aluminized Mylar
H_2O	190	10.9
CO_2	21	1.4
O_2	3.4	–
N_2	0.61	0.16
Xe	0.10	–
C_2F_6	< 0.01	–
CF_4	< 0.001	–

option is that the active chamber gas be diluted with a low-Z gas such that the buffer volume could be filled with CF_4, another gas that is relatively dense ($\rho_{CF_4}=$ 3.9 g/liter) and X-ray transparent. The reason that CF_4 is preferable to C_2F_6 is that the latter gas is more degrading to the chamber performance, if any were to accidentally leaked in. The response of a test chamber to small admixtures of these two Freons is shown in Figure 2.16.

Figure 2.17 shows the absorption lengths of C_2F_6 as a function of X-ray energy. For the lowest energy X-rays from transition radiation its absorption length is about 4-5 cm. To have the least effect on TR generated X-rays their path length it is best to minimize their path length. The estimate of the size of the buffer volume at its maximum width is approximately 1 cm.

Long term tests with a full size prototype

Tests were performed on a near full-size test chamber to determine the long term stability of the system. A chamber approximately 1.6 meters square was constructed from chambers that were a part of experiment E672. The anode-cathode gap was 9mm, the distance between cathode wires was 2 mm, and the distance between anode wires was 6 mm. The windows were constructed so that there was a front buffer volume, and the inner window was only 1.5-2 mm away from the cathode wires. The chamber was attached to the recirculating gas system, and checked out with an Argon-Ethane mixture. It was determined that the stability of the system was adequate, and the chamber was then filled with an 80% Xenon and 20% CF_4 mixture. The buffer volume was filled with a C_2F_6/CF_4 mixture that was equivalent in density.

During approximately 1 month of running with the Xenon mixture, the chamber performed remarkably well. An ^{55}Fe x-ray source was located at a constant

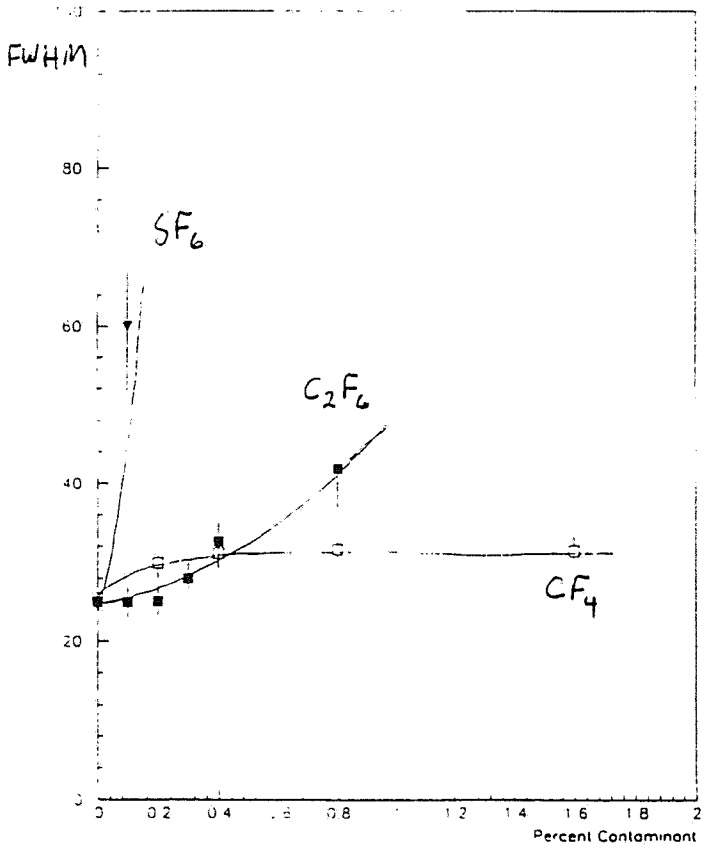

Figure 2.16: Resolution of test chamber with respect to admixtures of C_2F_6 and CF_4 and SF_6.

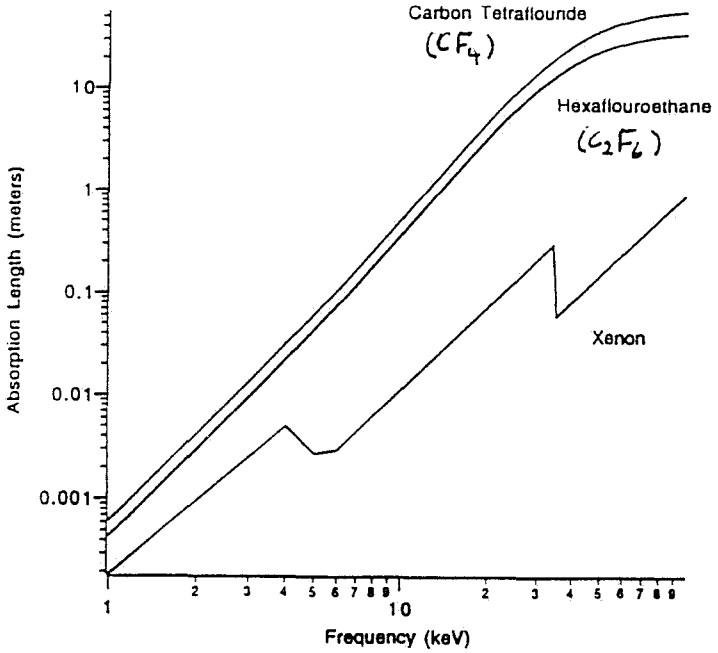

Figure 2.17: Absorption length vs X-ray energy for C_2F_6, CF_4 and Xe.

position and the chamber response was read out. Some adjustments to the gas system had to be made approximately 2 weeks into the run, at which point the system became very stable. Figure 2.18 shows the temperature corrected output of a position sensor. This data shows that, for a 17 day period, the gas system can hold the position of the inner window stable to within $\pm 50 \mu m$.

The raw output of the chamber response to the x-ray source is shown in figure 2.19a. Large fluctuations are visible in this response. However, as figure 2.19b shows, the atmospheric conditions are changing dramatically during this same period, so that the response of a gas chamber should fluctuate. Finally, figure 2.19c shows the chamber response corrected for the atmospheric fluctuations. All the major fluctuations are gone, leaving periods of very constant gain, followed by a small, rapid decreases in gain of about 4%. The small step changes in gain are correlated with times of large replacement of gas in the active volume, and either an introduction of contaminants or a change in gas mixture was taking place. Studies with the gas chromatograph of samples taken during the run show the evolution of the gas mixture with time. As the recirculating system ran the oxygen concentration dropped, the water vapor and CO_2 remained the same, nitrogen and C_2F_6 slowly increased, but the main cause of the decrease in gain is attributable to the increase in CF_4 from the mixing system modifications. Any changes in gain will be monitored during the

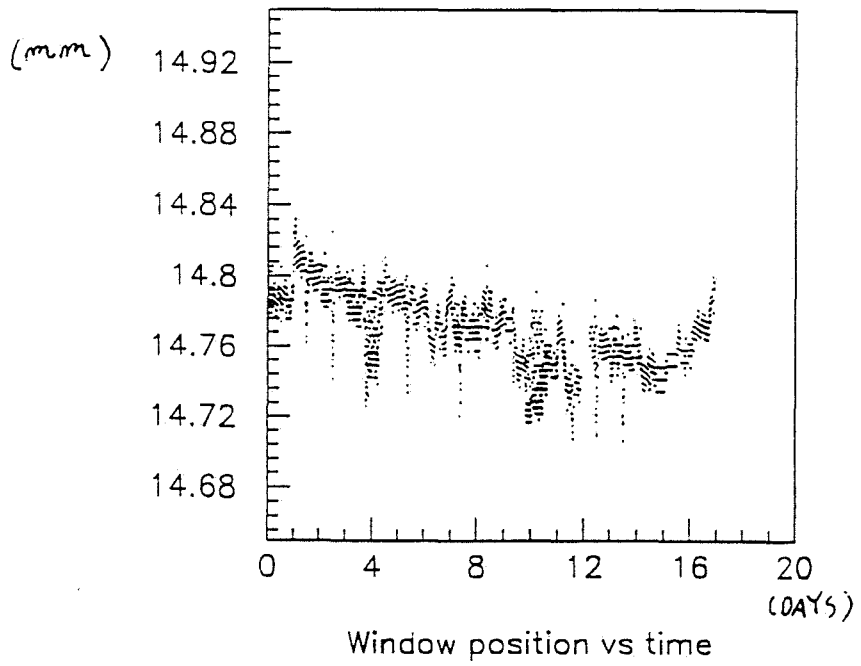

Figure 2.18: Temperature corrected position sensor output for a 17 day period of running with the large size prototype.

experiment, and compensated for by changes in the voltage of the chamber.

The gain of the prototype chamber as a function of the rate of incoming X-rays was checked after the long term test was over. Figure 2.20 shows the gain of the chamber as a function of the rate of pulses. The collimated beam of the X-ray source was on the order of 2-3 mm square. Therefore, a 1 kHz rate on this plot translates to an absolute rate of about 10 kHz per square centimeter. This is about the highest rate at KTeV. There is a significant dependence on rate (10-20% at 10 kHz/cm^2) that may need to be accounted for during the run.

2.3.3 Radiator design

Many distinct radiator materials were tested for π/e discriminating transition radiation detector at the KEK (Japan National Accelerator Laboratory, Tsukuba, Japan) electron test beam facility. They were tested using TRD prototype wire chambers built at Fermi National Accelerator Laboratory. Each chamber was a twin multi wire proportional chamber with an anode to cathode spacing of 6 mm. The chambers were filled with 90/10 Xenon/Methane. The radiators came in three different forms: foil stacks, fiber mats, and closed cell foams. All of the radiators under consideration were made from polypropylene. For the purposes of fair comparison, all of the radiators were constructed so that the length of each radiator was equal to one X-ray absorption length at 10 keV for that radiator. The value of 10 keV was chosen since simulation studies of the expected design of the KTeV TRDs have peak absorption at that X-ray energy.

At KEK, a 0.5 GeV to 5 GeV electron test beam was available for the radiator test. The data was taken with LeCroy 2249A ADC modules with a 300 ns gate. Triggers were provided by a pair of thin scintillator immediately upstream of the wire chambers required to fire in coincidence. Energy spectra were taken with each radiator at 5 GeV. For comparison purposes, data was taken at 5 GeV with a polypropylene plate that was also one x-ray absorption length at 10 keV. Since no transition radiation is produced by a simple plate, the spectrum from the polypropylene plate runs are a measure of the ionization energy deposit in the prototype chambers. To measure the absolute transition radiation energy spectrum, the chambers were calibrated using the 5.9 keV line of ^{55}Fe and the 19.6 keV line of ^{109}Cd. A normalized spectrum from the polypropylene plate was subtracted from each radiator spectrum to obtain the absolute transition radiation spectrum. Figure 2.21 compares data from a radiator run to that of a polypropylene plate run, and shows the transition X-ray spectrum obtained.

Figures of merit of the different radiator samples are obtained by normalizing the number of triggers in the polypropylene plate spectrum to the number of triggers

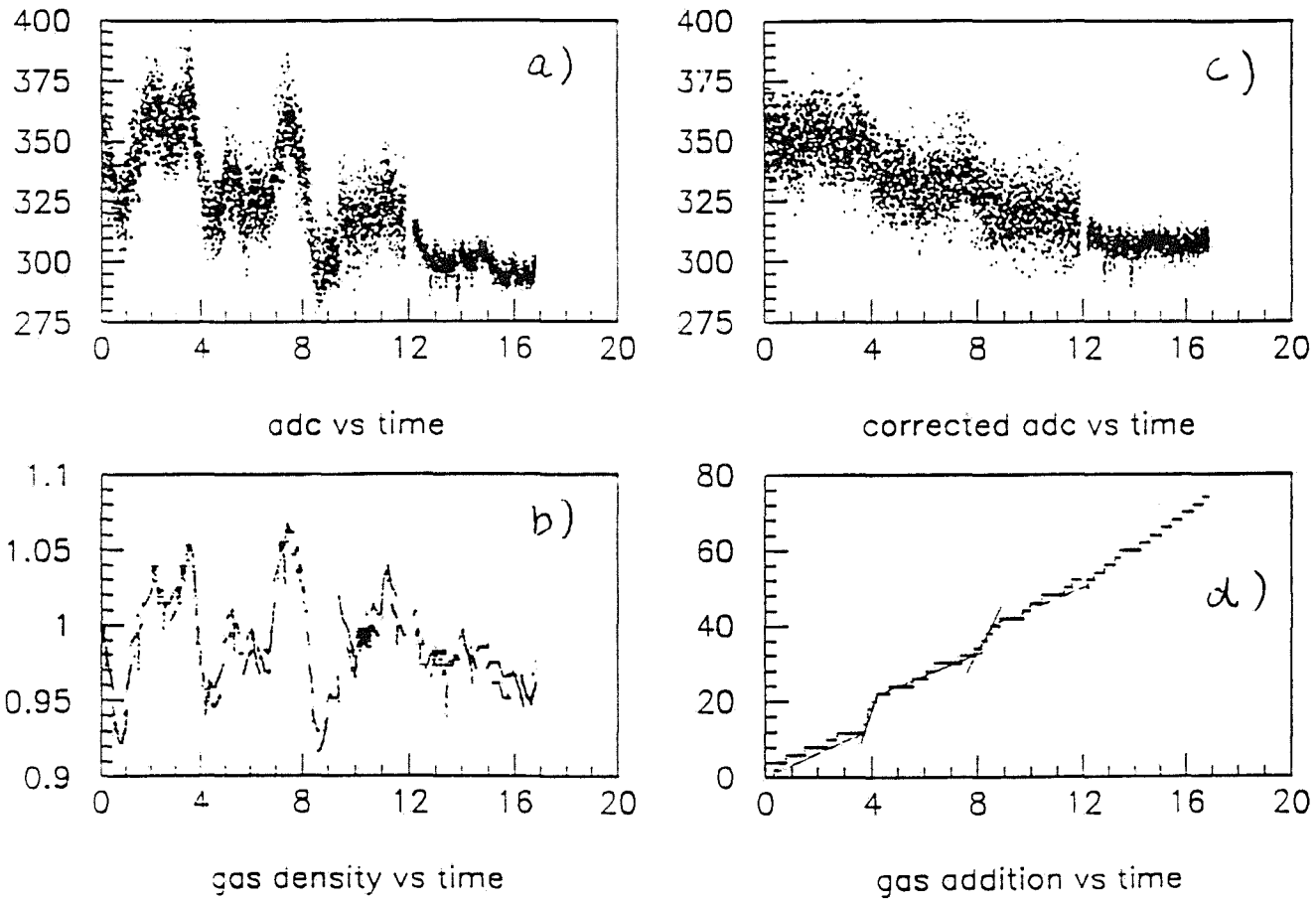

Figure 2.19: The raw chamber response for a) the 17 day period of the large size test chamber, b) shows the inverse gas density during this same period, as calculated from atmospheric pressure and temperature, c) shows the gas density-corrected chamber response for the same period, and d) is the number of gas injections into the chamber for this period.

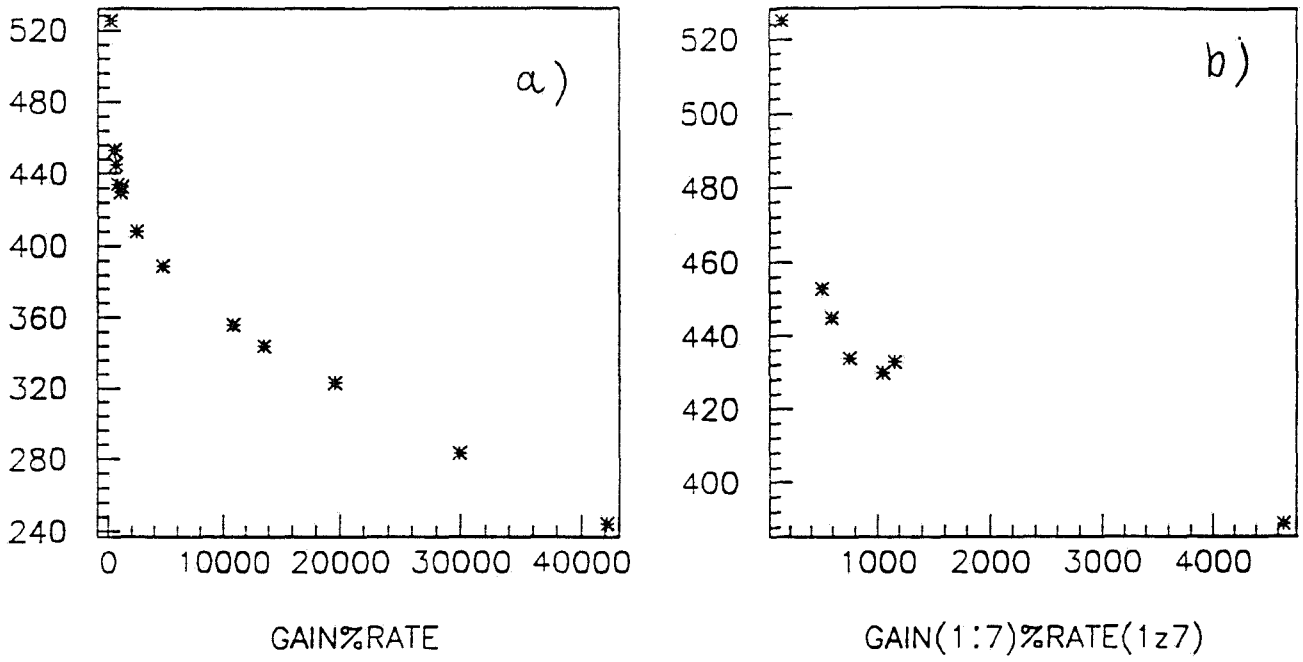

Figure 2.20: The response of a test chamber to a) a collimated x-ray source as a function of the pulse rate in the chamber, and b) details of same; both scales are in Hz.

Table 2.4: KEK results on radiator performance

Radiator material	Figure of merit
Foil stack	.276 ± .016
LASR fiber mat	.333 ± .016
Triumph fiber mat	.300 ± .015
E799-I fiber mat	.289 ± .015
Venus fiber mat	.220 ± .015
2.2 Polyplank foam	.250 ± .017
4.0 Polyplank foam	.178 ± .015
6.0 Polyplank foam	.083 ± .018
9.0 Polyplank foam	.078 ± .018
31. Rohacel foam	.170 ± .019
110 Rohacel foam	.122 ± .017
170 Rohacel foam	.097 ± .019

in each radiator spectrum. The cut off energy of the absolute transition radiation spectrum is used as a threshold point. The percentage of events in the radiator spectrum above this threshold minus the percentage of events in the polypropylene plate spectrum gives the figure of merit. The figure of merit is an estimate of the number of of electrons accompanied by at least one transition radiation photon, in percent. Table 2.4 shows a list of radiator samples with their final figures of merit. The best radiator appears to be the LASR fiber mat.

The final design of the radiator will use the polypropylene fiber mat, one of the test TR materials found. This fiber will be supported in a box made of thin-walled, low-density polypropylene foam, approximately 1/2" thick. The total depth of the box and fiber within will be 0.125radiation length. There will be two holes made in the radiator, each 15.5 × 15.5 cm^2, to let the two neutral beams pass. Mechanical supports for these fiber-boxes will be attached to the walls of the strong-back of the chamber. Since these fiber-boxes are very light (on the order of 100 kg), no major difficulties in mounting them are envisioned.

2.3.4 Electronics

The current design for the TRD electronics has the signal coming from the chamber into a preamplifier mounted directly on the chamber. A design similar to that

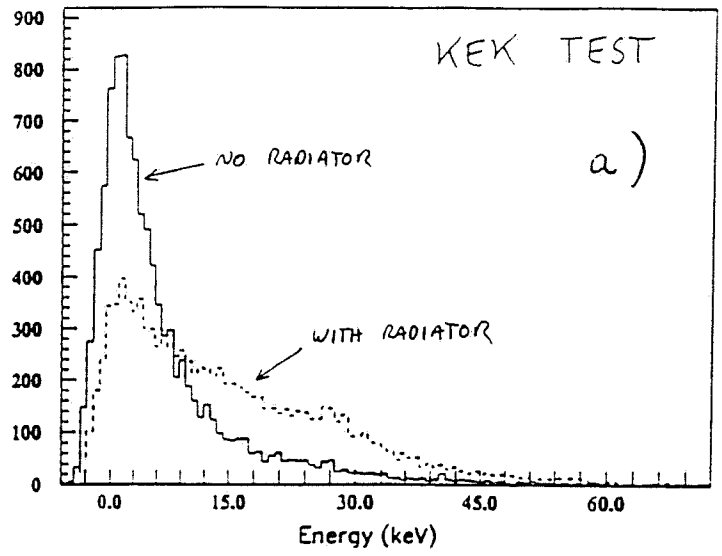

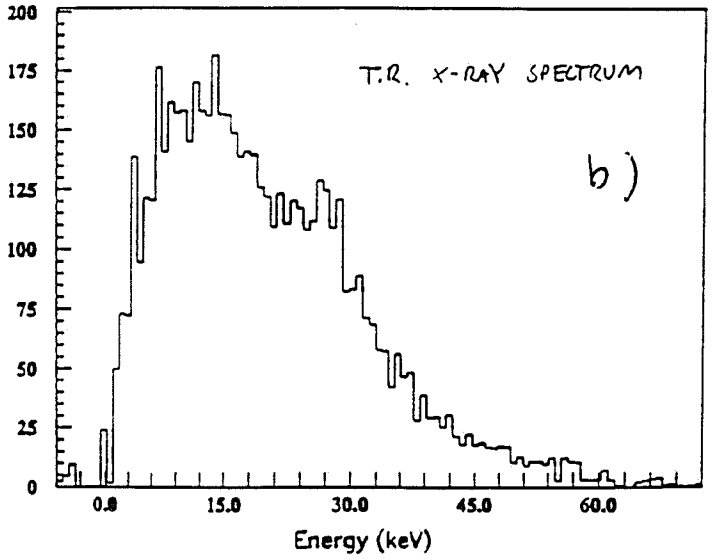

Figure 2.21: Part a) shows a comparison of energy spectra using a radiator versus using the polypropylene plate in front of the test chamber. b) is the difference between these two spectra, which can be attributed to transition radiation.

used in E799-I is planned. The output of this pre-amp is a differential signal, with 16 signals coming from each pre-amp card. The differential signal will be carried along twist/flat ribbon cable to another receiver and shaping amplifier, which can be located a distant from the TRD chambers and closer to the ADCs in the counting room. The output of this amplifier goes to the ADCs through a lead of ribbon coax signal cables. The secondary amplifier cards can be located at a convenient location within a 50 ft area from the TRDs themselves.

There are two designs currently being looked into to form an electron trigger from the TRD system. The first one employs LeCroy ECLine logic modules and the second one can be a custom made discriminators incorporated into the receiver amplifier. In either case, one likely needs to use low threshold discriminator hits to define a particle path. Then, along this path, one defines whether the track itself is an electron or a pion by counting the number of high threshold discriminator hits. Because of the moderately long gate width of the TRD signals, the planes will be susceptible to a high accidental activity, so it seems necessary to define these particle paths from ionization signal alone, and that a majority logic of the sum of the plane signals would not be adequate. It is envision that only the front wire plane of each chamber will be used for this trigger; since analysis shows that the rejection power of the front plane is higher than the rejection power of the sum of the front and back plane. More trigger studies are necessary to address how much rejection can be obtained from this trigger. The granularity of the paths will be defined by Monte Carlo study. The potential gain in physics for the experiment of a TRD trigger justifies its presence if it can substantially reduce the level 2 trigger rate. A mode detailed KTeV note explicitly laying out the design of the full TRD electronics system will be prepared.

Table 2.5 shows the sources of delay required for the TRD signal. The total comes to 465 ns, and a total signal delay of 500 ns was chosen for the system. This delay is equivalent to approximately 330 feet of cable. Some of this delay will be in delay from the pre-amp on the chamber to the post-amp card, where the signal is differential. This cable can be twist and flat, 17 pair cable, which comes in 100 foot lengths. This leaves 230 feet of cable which can transmit a signal with a minimum loss or degradation. Ribbon coaxial cable would be ideal, but is too expensive–on the order of $100,000 for all cable required. Another option is individually shielded twisted pair, which comes 17 pairs per cable. This type of cable was used in E799-I, which means that about 600 channels are available free of charge if the same type of cable can work. Purchasing the required length for all 2000 channels would cost approximately $58,000 for this cable.

2000 channels of FERA ADCs are avaliable for use by the TRD system. These will be located in approximately 10 CAMAC crates in the counting room. They will

Table 2.5: Required signal delay for TRD system

Source of delay	Amount (ns)
Level 1 Trigger	350
CsI PMT	25
Position of TRD	20
Gate inside ADC	20
Trigger to ADC	50
Total	465

be read out through DYC+ interface modules, one per crate.

2.3.5 Monitoring of Detector

During operation of the detector both the gas mixture and chamber gain will be continuously monitored by independent systems. To keep a high level of stability in chamber gain the high voltage will be adjusted to maintain a good pion rejection and stable X-ray pulse heights for triggering.

Monitoring the gas mixtures

For the precise control of the gas composition and possible accumulation of impurities a gas chromatograph will be used to periodically monitor the gases. This gas chromatograph consists of a carrier gas system, injection system, an oven containing a column, and a detector. A carrier gas of ultra pure helium is being used. The injection system allows the introduction to the Helium carrier flux a small volume of sample gas (50 μliters). The column is a capillary tube filled with an absorber material. The detector measures the concentration of impurities in the carrier gas. When a gas mixture is injected into the column it experiences adsorption and this affects its arrival time into the detector. Different gases have different adsorption coefficients and therefore different arrival times. As a result, by recording the signal from the detector in time one can resolve different components in the analyzing mixtures.

The sensitivity of the gas chromatograph is demonstrated in 2.22, in which a chromatogram is presented of a standard He gas (He100), containing only 50ppm of impurities. From the retention times one can clearly identify some particular

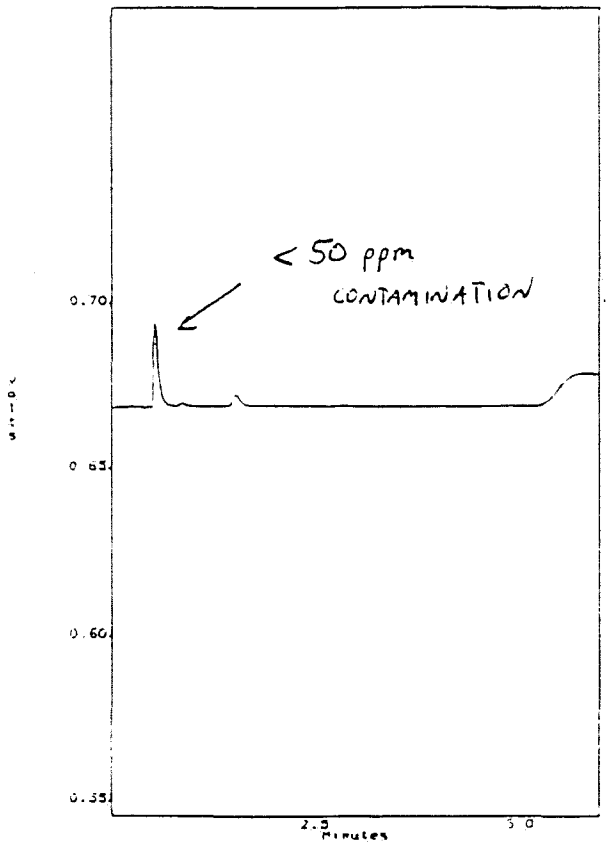

Figure 2.22: A demonstration of the sensitivity of the gas chromatography setup to impurities at the level of 50 parts per million.

impurities as: N_2, O_2, C_2F_6 and H_2O. Figure 2.23 shows a chromatogram of the gas mixture Xe/CF_4 used in the large size prototype detector. Besides the Xe and CF_4 peaks, one can see also peaks of N_2 1200±43 ppm, O_2 200±70 ppm, H_2O and C_2F_6 144±43 ppm.

Gain Monitoring and High Voltage Control

Each detector will have a low level X-ray source mounted in the corner of the detector to monitor and control gain variations caused by atmospheric pressure or gas composition changes. Because the rejection power of a TRD is susceptible to gain variations mainly due to changes in the X-ray pulse height gain, monitoring and control is necessary. Using a computer-programmable high voltage system, such as the CAEN SY127 wire chamber system, permits monitoring of all chamber voltages

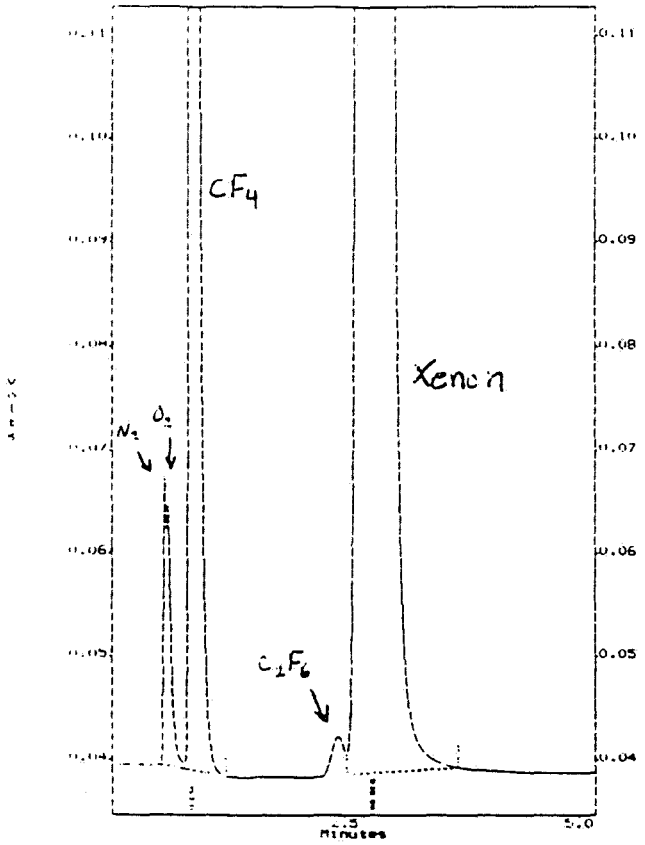

Figure 2.23: A chromatogram of a sample of the gas mixture used in the large scale prototype.

and currents and can easily be programmed to compensate for gain drops. An independent computer system with a data acquisition system can monitor the X-ray peak on the side wires near the source and periodically adjust the high voltage in this system to keep the gain stable at the 10% level. This will also make the TRD electron trigger stable at a similar level.

2.4 The TRD System

The TRD system combines the operation of the individual detector planes to do electron identification. For the KTeV E799-II rare kaon decay program to be successful a minimum system performance of 200:1 pion rejection is needed. The number of individual detectors and radiators has been studied considerably to evaluate potential performance. A CERN beam test is scheduled for April 1994 to determine the final rejection power of our system and confirm the number of detector planes needed.

2.4.1 Number of chambers

Results on the TR X-ray production and ionization studies have allowed the development a program simulating the full TRD performance to determine the number of chambers needed in KTeV to reach 200:1 pion rejection. If the number of chambers in the TRD system is increased while keeping the radiator size per chamber constant, the rejection factor will increase exponentially if material losses are neglected. However, if the total amount of radiator material in the TRD system is kept constant while the number of chambers is increased, the rejection factor levels off at 6 to 8 chambers (Fig. 2.24). The onset of this plateau is independent of the exact amount of radiator material, but the total amount of radiator material does affect the actual rejection power. The value of rejection with this number of chambers, for a total radiator thickness of 10% of a radiation length, is 200 to 400. The rejection factors here are for 90% electron efficiency.

2.4.2 Pion rejection studies at BNL beam test

A beam test of the three experimental chambers built by Fermilab was conducted at Brookhaven National Laboratory from 6-9 July, 1993. The B2 beam line at BNL was used, which consisted of a minimum bias, momentum-selected secondary beam. The momentum bite was approximately 1%, according to calorimetric analysis of the beam. The beam was tuneable from 0.5 GeV to 8 GeV, with the electron fraction of the beam decreasing steadily with energy. Two Cherenkhov counters containing Nitrogen were used to distinguish electrons from other minimum ionizing particles (identified as 'pions' hereafter). This identification worked more efficiently

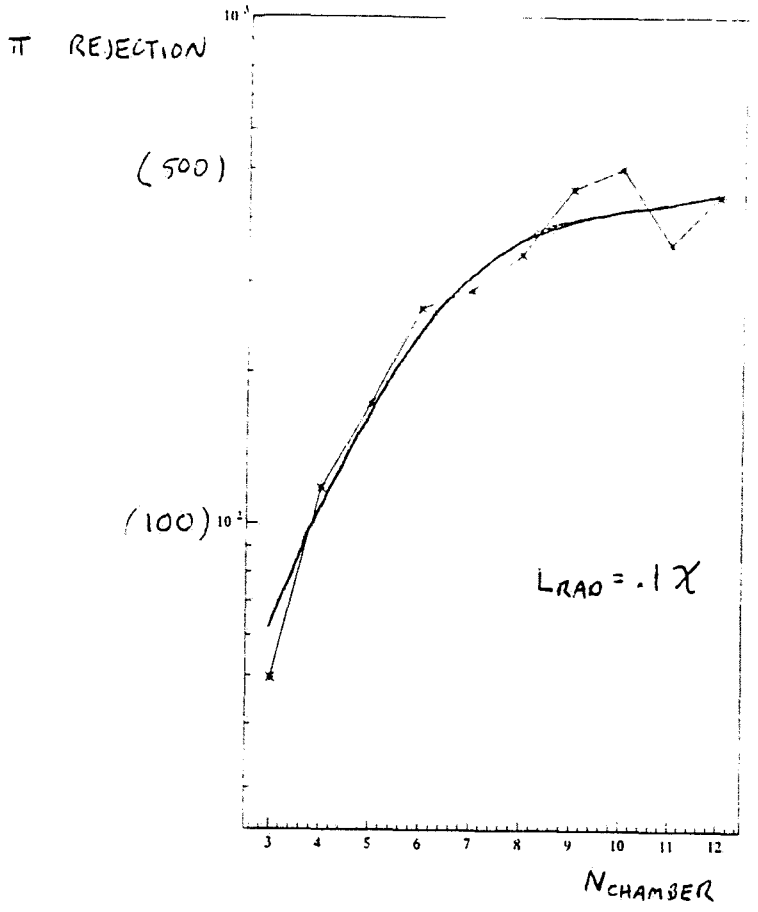

Figure 2.24: Pion rejection as a function of the number of chambers in the TRD system, given a fixed amount of radiator.

for particles with less than 5 Gev in momentum. A beam particle trigger was created from the coincidence of two scintillator paddles set in front of the detectors. The signal from one Cherenkhov detector was discriminated and used to form a trigger for electrons.

Figure 2.25 shows the comparison of the sum of signals from all wires in a chamber for particles identified as electrons vs that from pions at 4 GeV. A cut has been made on the data to ensure that only 2 or 3 wires were hit in the event; remembering that a track will always hit a wire in each of the two planes. A clear difference is seen in the two distributions. Also in this the figure are plots of the efficiency for passing the electron signal vs the efficiency for passing the pion signal for various cuts on signal size, where efficiency is defined as the fraction of events passing a given cut. The solid lines in these efficiency plots are equal rejection lines for 70 % electron acceptance in a 10 chamber system. These plots indicate that a 10 chamber system would give a factor of 100 rejection, but only at 70 % acceptance.

The previous analysis is poor at estimating the rejection from the TRD system. This is because summing up all the wires means that an ionization signal will show up twice, one for each layer, but if there is only one transition radiation X-ray, then the TR signal will show up only once. Realizing this a reanalysis of the Brookhaven test beam data was performed with a 2-dimensional likelihood analysis. Figure 2.26 show the 2 dimensional scatter plots of 2 GeV data, with the response of the chamber's front layer plotted against the response from the chamber's back layer. Note the significant difference between the pion and electron samples. For the electron sample there are many events with a large response in one of the two layers, thus indicating that there is probably a single transition radiation X-ray in that event. There is a smaller number of events where there is a large response in both layers, possibly indicating an event with 2 X-rays. The likelihood is determined by normalizing the contents of the 2-dimensional scatter plots to unity, and then determining the probability associated with each bin in that scatter plot. By looping over a number of events and multiplying the respective probabilities, one obtains the likelihood for a pion and electron. Figure 2.27 shows the log-likelihood comparisons with 8 events (simulating 8 chambers) and the pion rejection as a function of the electron acceptance. Here we can see a factor of 100 pion rejection, with only 8 chambers, at an electron acceptance of 90%. This is a very large improvement over the single dimensional value, and is indicative of the capabilities of the final system. As mentioned, this value of rejection is lower than the Monte Carlo estimate since the test chambers did not have an active drift region at the front of the chamber.

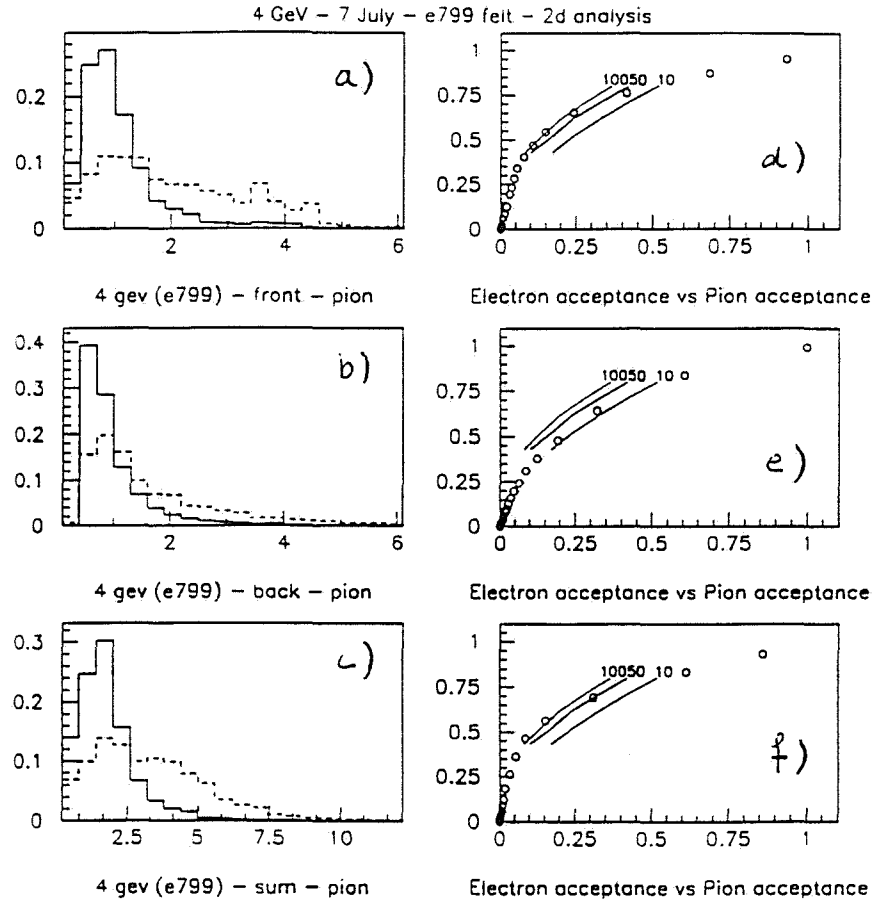

Figure 2.25: A comparison of signals in a test chamber to electrons (dashed) and pions (solid). a) is for the front layer of wires, b) is for the back layer of wires and c) is for the sum of all wires. Graphs d), e), and f) show the rejection from this data for 70% electron acceptance for 10 chambers.

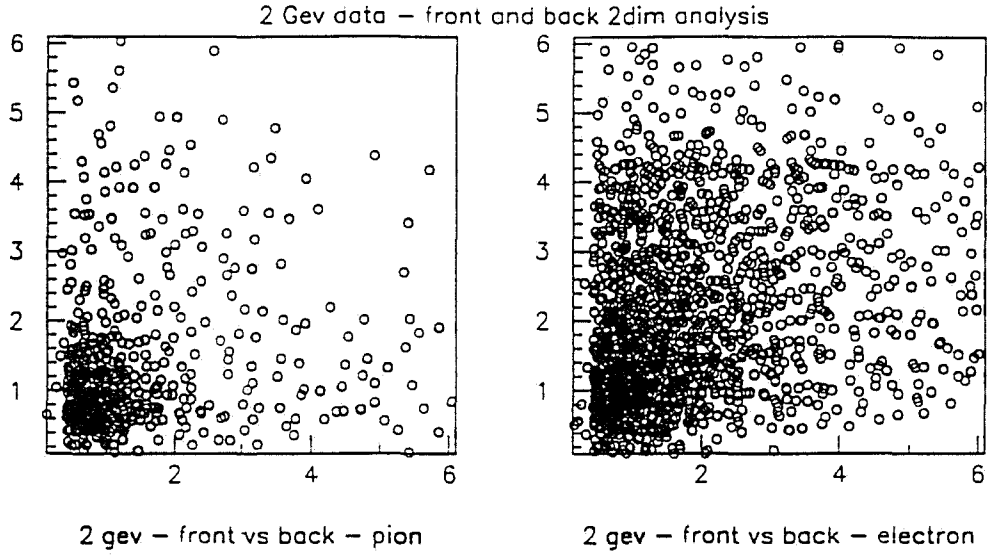

Figure 2.26: Parts a) and b) are the scatter plots of front layer energy vs back layer energy for the pion and electron data sets, respectively, at 2 GeV, for a test chamber with LASR fiber as radiator.

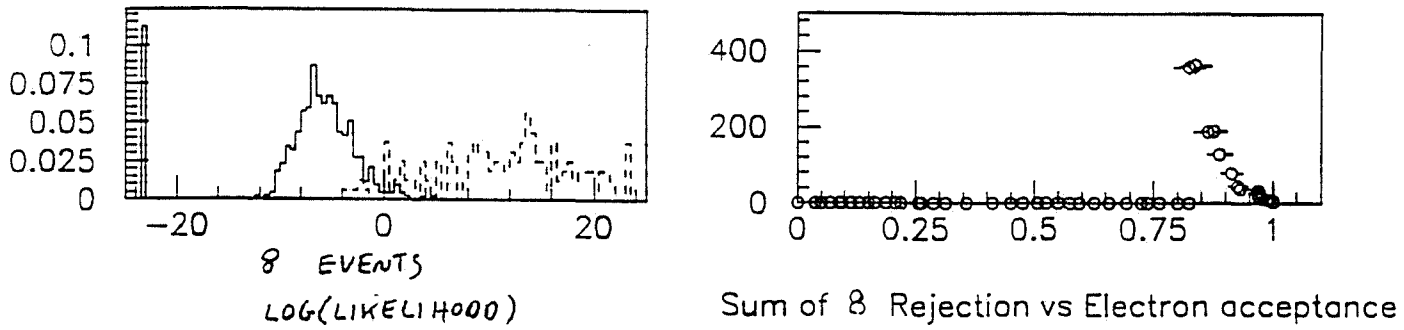

Figure 2.27: Part a) shows the comparison between the log(likelihood) for being an electron in the pion sample (solid) vs the electron sample (dashed), using 8 events, b) the amount of pion rejection obtained from these graphs, as a function of the electron acceptance. Zero values indicate indefinite rejection.

Chapter 3

Engineering details of the design

A cross sectional view of a fully constructed TRD chamber is shown in 3.1. As described in the previous section each TRD actually consists of two independent MWPC detectors with an active area of 1.8 m x 1.8 m and a clear aperture of 2.1 m x 2.1 m inside the frames. Wire plane cathodes will be used to decouple chamber gain from gas window position. The 2.5 mm cathode wire spacing is small enough to reduce the sensitivity of chamber gain to gas window motion by a factor of ten. The inner gas windows are operated at a more negative potential than the cathodes, so electrons from any X-rays which convert in that 1.5 mm gap will drift into the MWPC and produce a signal. The anode to cathode gap is 6 mm, the smallest practical size based on chamber building technology at Fermilab.

3.1 Construction of the wire planes

Each wire plane consists of a lamination of fiberglass and steel. A steel core of 1/8" thickness will be laminated on one side with plain fiberglass, and on the other side with copper coated fiberglass. The copper coating will be etched away to produce signal traces. The plain fiberglass side will be milled, or otherwise fabricated, so that the two opposite surfaces will be parallel to within approximately 50 μm. The frames have holes located periodically, so that clamping bolts can be used to close the chamber. Gasket sealer will be used between the frames to form the gas seal. A strong-back made of tubular aluminum will be machined on one face to form the backbone of the chamber, while channel aluminum on the opposite face will form the clamping frame. A blueprint for one of the frames is shown in 3.2.

The original plan for fabricating the frames for the TRD wire planes and gas windows involved a three step process employing two vendors outside of Fermilab. First, an outside vendor would fabricate cores from 1/8" thick by 8" wide strips

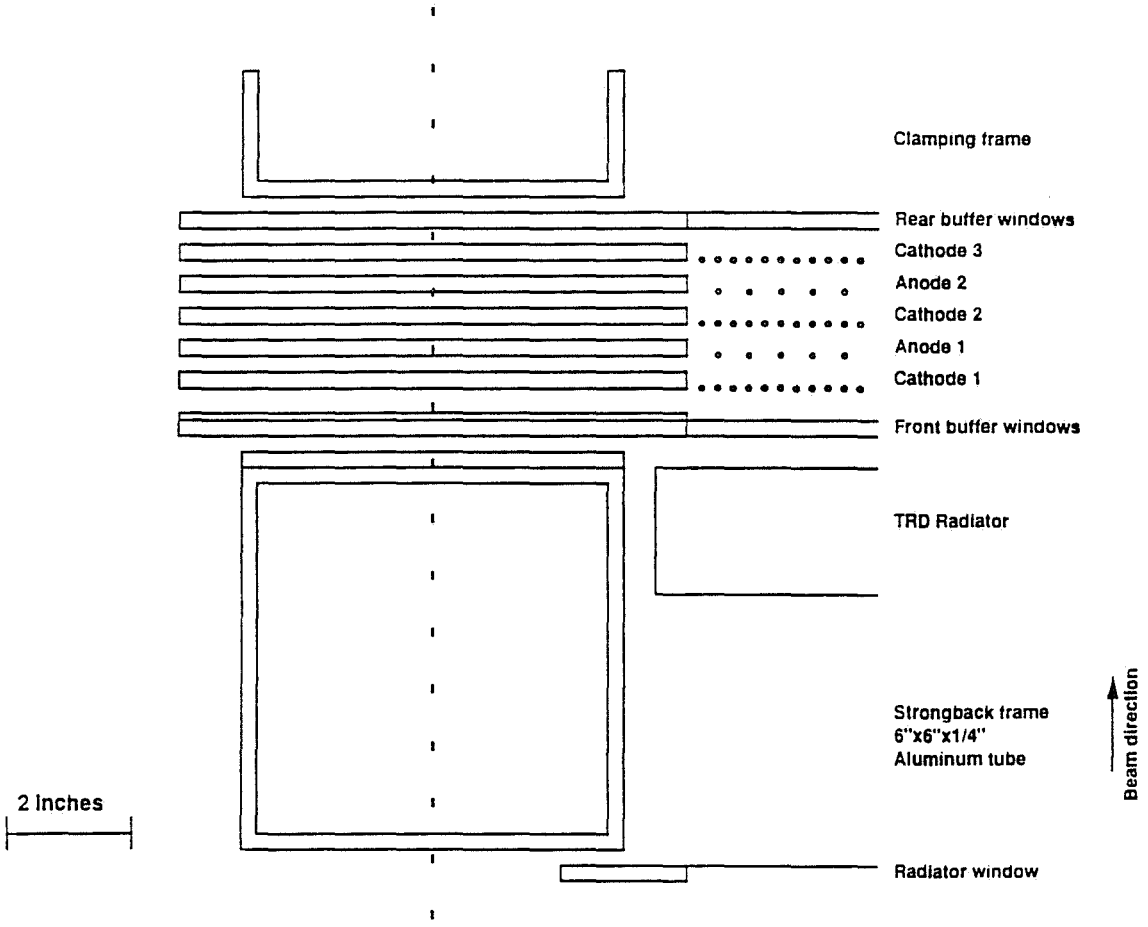

Figure 3.1: A cross sectional view of a TRD chamber.

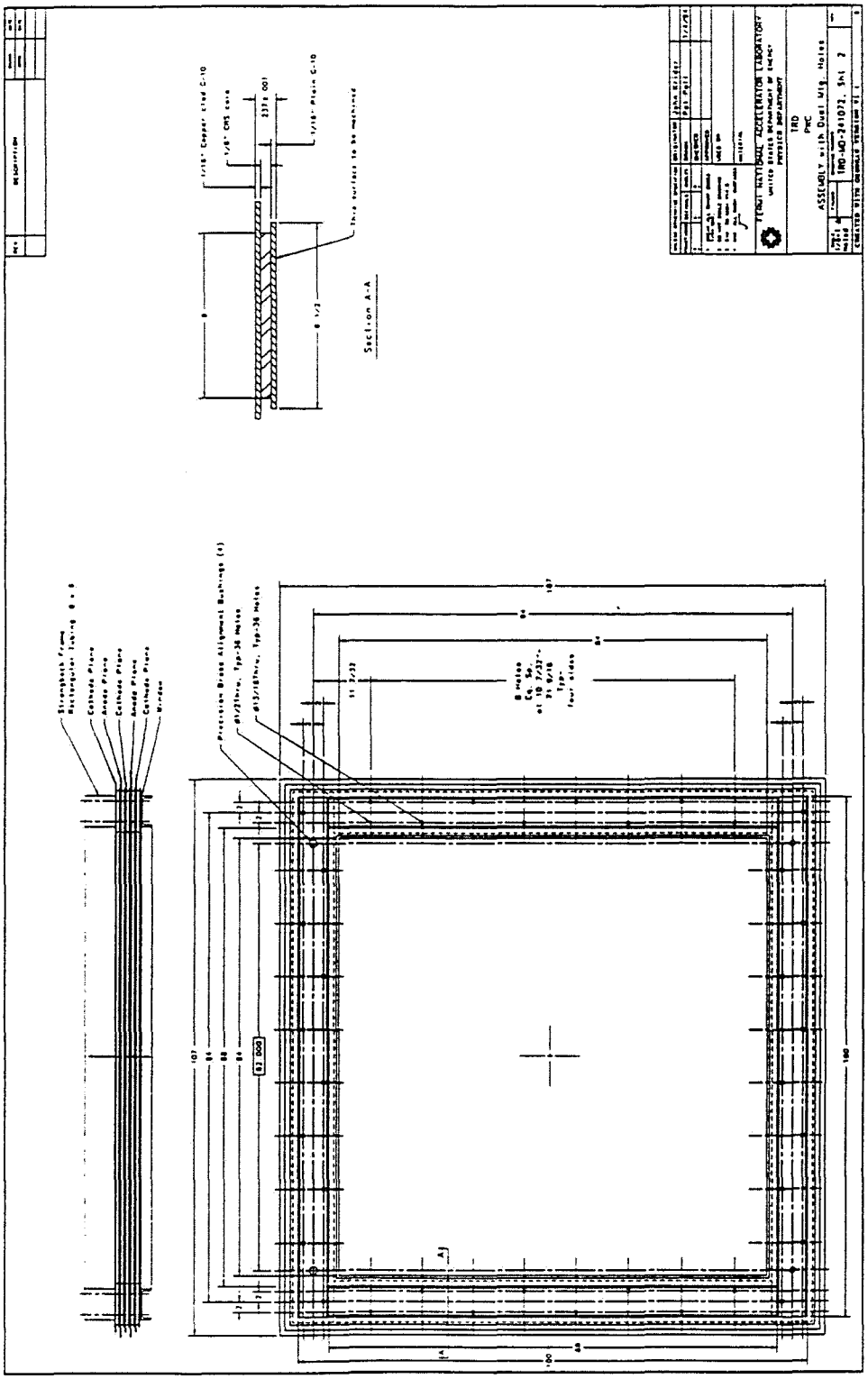

Figure 3.2: Engineering drawing for a TRD wire frame

of cold rolled steel by preparing and welding the corners. Then Fermilab would laminate 1/16" thick layers of FR4 (fire retardant version of G10) onto the metal cores without careful attention to overall thickness. Finally the laminations would be sent to another vendor for drilling and planing to about ±0.002" thickness tolerance. Disadvantages of this method include the high cost of outside labor and the scheduling delays resulting from outside vendors requiring that their part of the work be done in a few large batches. Since we produce the laminations and do the wire winding in a slower serial fashion, using outside vendors will not permit us as much freedom in interleaving the laminating and winding operations.

While we are awaiting bids for core fabrication and lamination machining, we are evaluating an alternative lamination method that could eliminate the outside operations, and should not significantly increase in-house labor. This technique would clamp the laminating layers between two tooling plates separated by precise thickness spacers. A thin layer of open cell foam would be included between the core and one or both layers of FR4. The foam density and thickness would be chosen such that it would provide sufficient pressure to hold the outer layers against the tooling plate at all points. Overall thickness should then be as accurate as the parallelism of the tooling plates. The corners of the core material would be mitered, and 8" x 8" x 1/16" metal cover plates would be laminated over the corners to provide strong joints. A small frame is currently being assembled from 6" wide by 30" long strips of materials to evaluate this alternative laminating technique. If this works, a full sized frame will be attempted.

3.2 Tolerances

Considerable attention has been give to mechanical construction tolerances and to system operating conditions, with a goal of ±25 % in uniformity and long term stability of gain. The wire plane support frames will be machined and assembled to provide an anode to cathode gap tolerance of ±50 μm around the perimeter, which produces gain variations of ±10% across a plane. Anode wire pitch variations of ±25 μm contribute another ±6 %. Electrostatic forces on the outer cathode wire planes will cause them to deflect inward toward the anodes by about 100 μm at the center, producing a gain variation of 10 %. Channel to channel electronics and cable variations are likely to contribute another 10%. The principal contributions from the gas system are (1) 3 % changes in atmospheric pressure or temperature producing gain changes of 10% each, (2) a 1 % change in the gas mixture ratio producing 10 % change in gain, and (3) contamination by modest amounts of O_2, H_2O and C_2F_6 can produce a 10 % reduction in gain.

The chambers have double gas window construction to provide buffer volumes.

These buffers reduce permeation of atmospheric gases into the active gas system, and they eliminate hydrostatic bulging of the inner windows, if the active and buffer gas densities are matched. The windows are stretched with a tension of 15-20 N/cm, and their resulting deflection constant at the center is about 20 μm/mTorr of differential pressure. This buffer volume is part of the entrance window for the X-rays, and therefore must be highly transparent above 4.5 keV.

3.3 Possible future extensions to the design

The design presented in this document is an achievable design that will meet the requirements of KTeV, within an achievable budget. However, this design is also flexible enough to be improved for future applications. For example, even though we are reading out at most only every 1 cm, the anode wires themselves are pitched every 5 mm. If every wire were read out, this would reduce any accidental background by at least a factor of 2, and would increase the rejection of the system. We have also learned from simulations of the detector that a significant increase (possibly more than an order of magnitude) in pion rejection can be made by using three layers of wire planes instead of two. If funds become available, this would be a very good way to increase the performance of the TRD system. The cost of such an upgrade would be dominated by the additional electronics involved. The geometry of the chambers can easily accommodate a third layer of anode wires.

3.4 Manpower

Physicists, engineers and technical support people currently involved in the design, R&D, procurement and construction of KTeV TRD system are listed below.

- Physicists

    1. Yee Bob Hsiung, Fermilab - Physics (System Manager)
    2. Erik Ramberg, Fermilab - Physics
    3. Robert Tschirhart, Fermilab - Physics
    4. John Krider, Fermilab - Physics
    5. Valadmir Peskov, Fermilab - RD
    6. Greg Graham, U. Chicago
    7. Nick Solomey, U. Chicago
    8. Yau Wai Wah, U. Chicago

9. Eric Zimmerman, U. Chicago

- Engineers

  1. Carl Lindenmeyer, Fermilab - Physics
  2. Dave Pushka, Fermilab - RD (KTeV Project Engineer)
  3. Harold Sanders, U. Chicago

- Technical

  1. Karen Kephart, Fermilab - Physics (Lab6 Winding Facility)
  2. John Korienek, Fermilab - Physics (Procurement)
  3. Pat Poll, Fermilab - Physics (Design/Drafting)
  4. Sharon Strecker, Fermilab - Physics (Lab6)
  5. Donna Hicks, Fermilab - Physics (Lab6)
  6. Brian Lavoy, Fermilab - Physics (Assembly)
  7. Gene Beck, Fermilab - Physics (Assembly)

The TRD chamber construction will make use of the Chamber Wire Winding Facility in Lab 6 (Karen Kephart's group) to wind each wire plane, and the chamber assembly and test will be done in the Clean Room of Lab 7. During the construction phase two full time physicist will be required. The wire winding machine requires four operators, but this is only a half day job subsequently requiring two full time equivalent technicians. The TRD assembly requires two full time technicians. Testing of finished detectors will require two physicist. During electronics construction two electronic technicians (at the University of Chicago) will be required to stuff the boards.

3.5 Schedule and Cost

Figure 3.3 shows an estimate for a timetable for construction of the chambers for the TRD system. The completion of the system would occur on roughly the same time frame as beneficial occupancy of the KTeV detector building. Space has been reserved at the Muon Lab for staging of TRD chambers. As each chamber is completed, it will be checked out in the clean room of Lab 7, before shipping to this staging area.

Table 3.5 gives an estimate for the remaining cost of the TRD system. Cost of the front end FERA electronics is not included. A supply of gas has not been

Month -->	J	F	M	A	M	J	J	A	S	O	N	D	J	F	M	A	M	J	J
Task	94	94	94	94	94	94	94	94	94	94	94	94	95	95	95	95	95	95	95
Freeze mechanical parameters	X																		
Mechanical design	XX	XX	XX	XX															
Circuit design		XX	XX																
Procurement		X	XX																
Circuit fabrication TRD1 (10)				1															
Frame fabrication TRD1 (7)				1															
Frame lamination TRD1 (7)					1														
Frame machining TRD1 (5)						1													
Wire winding TRD1 (5)							1												
Window stretching TRD1 (4)							1												
Mainframe fabrication TRD1					1														
Mainframe machining TRD1						1													
Final assembly TRD1							1	1											
Testing TRD1								1	1										
Frame fabrication TRD2-8						2	3	4	5	6	7	8							
Frame fabrication TRD2-8						2	3	4	5	6	7	8							
Frame fabrication TRD2-8							2	3	4	5	6	7	8						
Frame machining TRD2-8								2	3	4	5	6	7	8					
Wire winding TRD2-8									2	3	4	5	6	7	8				
Window stretching TRD2-8									2	3	4	5	6	7	8				
Mainframe fabrication TRD2-8							2	3	4	5	6	7	8						
Mainframe machining TRD2-8								2	3	4	5	6	7	8					
Final assembly TRD2-8									2	3	4	5	6	7	8				
Quality control TRD2-8										2	3	4	5	6	7	8			
Testing TRD2-8											2	3	4	5	6	7	8		
Staging at New Muon												2	3	4	5	6	7	8	
Installation																	XX	XX	XX

Figure 3.3: A preliminary timetable for construction, testing and installation of the KTeV TRD system.

included in this cost estimate since it is considered here to be part of the operational cost of the system.

A quote of $3.55 per liter has been made for a research grade of Xenon and there are indications that a lower price can be obtained. At this price, a gas recirculating system is required for the active gas mixture to keep costs at a reasonable level. A system of 8 chambers entails a volume of 1600 liters. It is desirable to purchase on the order of 5 times this amount, 8000 liters, or about $30,000. The volume of the buffer region is several times smaller, $\approx$500 liters for the entire system. The latest quote on prices for C_2F_6 is approximately $0.50 per liter. Costs for this gas would be minimal if a simple recirculating system was built for the buffer volume as well.

The mechanical construction of 8 chambers and a support stand will be needed in 1994. Enough electronics for a single chamber must be built during this year as well, so we take 1/8 of the total electronics cost as necessary for 1994. Costs for the radiator, the cable, and the rest of the electronics can be put off until 1995. With a 20% contingency built in, our requirements for funding are:

1994: $146,250
1995: $140,550
1996: $30,000 (Operations)

Item	# of Units	Cost/Unit ($)	Total Cost ($)
CHAMBER CONSTRUCTION			
Wire frame material	60	400	24000
Frame welding/machining	60	600	36000
Strong-back material	8	500	4000
Strong-back machining	8	2000	16000
Gas manifold sets	8	1000	8000
Connectors	400	20	8000
Mylar		0	
Wire		5000	5000
System support structure		8000	8000
Subtotal			109000
Contingency			21800
Construction total			130800
RADIATOR CONSTRUCTION			
Radiator material		5000	5000
Support structure	8	500	4000
Subtotal			9000
Contingency			1800
Radiator total			10800
GAS SYSTEM UPGRADES			
Shutoff valves/couplings	32	250	8000
Misc. fittings/controls		10000	10000
Subtotal			18000
Contingency			3600
Gas system total			21600
ELECTRONICS			
Pre-amp electronics	2000	13	26000
Post-amp electronics	2000	10	20000
Crates, power supplies	10	500	5000
Trigger			0
Pre-amp cable	13K'	0	0
Signal cable	29K'	2	58000
Subtotal			103000
Contingency			20600
Electronics total			123600
GRAND TOTAL			286800

Table 3.1: Estimate of costs for completion of KTeV TRD system.

Appendix A

Listing of TRD documents

The TRD group has documented much of the information in this design report in a series of KTeV or internal memos. Here is a listing of the memos contained in this library. Copies of any of these papers can be obtained from the TRD group.

KTeV #	Date	Author	title
(internal)	11/10/92	J. Krider	Sandwich panels for KTEV TRD cathodes
(internal)	4/15/93	J. Krider	KTEV TRD schedule
142	7/19/93	Y. Wah	KTEV TRD ADC channel summary
151	8/19/93	All	Design considerations of the KTEV TRD chambers
152	8/19/93	M. Daum, *et.al.*	Description of test of KTEV TRDs at BNL and analysis
153	8/19/93	M. Daum, *et.al.*	Studies on gases for use in the KTEV TRD system
150	8/31/93	G. Graham	Calculated absorption lengths of various materials
146	8/17/93	G. Graham, *et.al.*	A study of TR X-ray yields from different materials
154	9/1/93	M. Daum, *et.al.*	Studies on TRD chamber windows
(internal)	9/6/93	G. Graham	The standard model TRD
155	9/10/93	M. Daum, *et.al.*	A 2-dimensional analysis of TRD test beam data.
(internal)	10/9/93	Y. Wah	Transverse size of the large KTeV TRD
(internal)	10/13/93	N. Solomey	Gain resolution studies with the three gas mixtures used
158	10/13/93	G. Graham	The radiation length of the TRD system
(internal)	1/24/94	N. Solomey	TRD electrostatic field calculations
164	11/24/93	N. Solomey	TRD entrance window design options
156	6/10/93	J. Krider *et.al.*	Xenon gas recirculating system for E799
166	11/24/93	G. Graham	X-Ray TRD simulation software
172	12/13/93	N. Solomey *et.al.*	X-Ray efficiency measurements with TRD prototype
180	1/28/94	G. Graham *et.al.*	Properly designing a conversion gap and entrance windo